QUANTITATIVE EVALUATION OF FLOW SYSTEMS, GROUNDWATER RECHARGE AND TRANSMISSIVITIES USING ENVIRONMENTAL TRACERS

E.M. ADAR
Water Resources Center,
Department of Geology and Minerology
Ben-Gurion University of Negev,
Sede Boker Campus,
Israel

Abstract

This chapter provides an overview of the basic concepts and formulations on the compartmental (mixing-cell) approach for interpretation of isotope and natural tracer data to arrive at quantitative estimates related to groundwater systems. The theoretical basis of the models and the specific solution algorithms used are described. The application of this approach to field cases are described as illustrative examples. Results of sensitivity analyses of the model to different parameters are provided.

INTRODUCTION

To properly manage groundwater resources, there is a need for accurate information about inflows (recharge), outflows (discharge) and the physical characteristics of aquifers. Yet, in many semi-arid and arid basins it has been common to exploit aquifers based on partial information about the hydrologic characteristics. A major source of uncertainty stems from the hydrologist's inability to reliably estimate the spatial and temporal distribution of recharge rates. Similarly, incomplete information of hydraulic conditions along the boundaries, such as fluxes and heads, imposes tremendous difficulties in aquifer numerical modeling. The difficulty is especially acute in semi-arid and arid regions where recharge is often occurs in pulses from floods of relatively short duration, and lasts from several hours to several days (Zimmerman, et al., 1966, 1967). In basins with limited number of wells and hence, limited knowledge of the hydrogeological structure, it is often difficult to precisely define the flow system or the boundary conditions. Furthermore, the lack of observation wells and pumping test data eliminate the possibility of proper calibration processes. For basins with a complex geological structure and with scarce hydrologic information, a method is introduced for a quantitative assessment of groundwater flow system, components of recharge, and transmissivities by incorporating environmental tracers such as dissolved minerals and isotopes.

Models that assess recharge by equating it to infiltration at the soil surface, (including stream beds), in response to rainfall, irrigation and stream flow abound in the literature. Examples can be found in the works of Eakin (1966), Feth, et al. (1966), Briggs and Werho (1966), Burkham (1970), Rantz and Eakin (1971), Belan (1972), Kafri and Ben-Asher (1978), Howard and Lloyd (1979), and others. Of particular interest for recharge from ephemeral stream losses in the

arid southern United States are the studies of Matlock (1965), Marsh (1968) and Keith (1981). Since not all the water infiltrated reaches the water table, the volume and rate of the water table recharge are generally less than those of infiltration. Only that water which actually reaches the water table, and in this way becomes part of the saturated zone, should be considered as recharge. For the computation of net input one needs to transform the infiltration into volumes or rates of deep percolation beneath the root zone, including the root zone of phreatophytes near streams and washes. Methods for effecting such a transformation have been described by numerous authors including Thornwaite and Mather (1957), Mero (1963), Walker (1970), Olmsted et al. (1973), Bos and Nugteren (1974), Heerman and Kincaid (1974), Wind and Van Doorne (1975), King and Lambert (1976), , Tanji (1977), Wilmot (1977) and Karmeli et al. (1978). While some of these methods may work well in humid regions, their applicability to semi-arid and arid conditions is in question.

Among the most readily available hydrologic data that one could use to estimate groundwater recharge in semi-arid and arid regions are stream flow records and hydrographs of nearby wells. Very often, the fluctuation of water levels in wells situated close to streams reflects fluctuation in the rate of recharge as well as the rate of deep percolation beneath the stream. The idea of using groundwater level fluctuations as an indicator of recharge dates back to the early work of Jacob (1943, 1944). Various methods based on this idea have been discussed by Wilson and DeCook (1968), Matlock (1970), Moench and Kisiel (1970), Venetis (1971), Matlock and Davis (1972), Gelhar (1974), Besbes, et al. (1978), Duffy, et al. (1978) and Flug, et al. (1980). When stream flow infiltration is the main source of recharge, some of these methods may yield acceptable results. However, none of the techniques mentioned thus far are able to deal with situations where the relative importance of diverse potential recharge sources is unknown.

In this work a methodology is developed for the identification and quantification of multiple recharge sources, subsurface fluxes, and aquifer physical parameters on the basis of hydrochemical and isotope data. This means using such data to elucidate the spatial distribution of recharge sources, flow components, and to estimate the relative as well as absolute strength of each such source. Under certain conditions this can be accomplished by solving an "inverse problem" of aquifer hydrology in which recharge is estimated jointly with the hydraulic parameters of a numerical aquifer flow model (Carrera and Neuman, 1986a, b & c). This, however, works only if the hydraulic properties of the aquifer are reasonably well characterized, and there is abundant information about its hydraulic response. While such information is often inadequate, data about groundwater chemistry and environmental isotopes can often be collected rapidly and at a relatively small expense. It is therefore important to examine the extent to which such data can be used for the identification and quantification of groundwater flow system.

In the past, hydrologists have used chemical and isotope data for recharge studies primarily in a qualitative sense. Environmental isotopes played a dominant role in such studies, as exemplified by the works of Verhagen, et al. (1970, 1978), Gat and Dansgaard (1972), Blake, et al. (1973), Bredenkamp, et al.

(1974), Mazor et al, (1974), Yurtsever and Payne (1978a & b), Shampine, et al. (1979), Levin, et al. (1980), Issar and Gat (1981), Issar and Gilad (1982), Mazor (1982) and Issar (1983). In some studies, tritium was used to obtain quantitative estimates of recharge (Dincer, et al., 1974; Bredenkamp, et al., 1974; Vogel, et al., 1974). More recent attempts to extract quantitative information about recharge from hydrochemical data often rely on statistical analyses. As an example, Lawrence and Upchurch (1982) use factor analysis to identify the recharge source for certain groups of dissolved chemical species in an aquifer. In all such works, the authors either evaluate the magnitude of a given recharge source, or evaluate the potential of recharge without providing quantitative estimates of recharge rates.

A serious attempt to incorporate hydrologic and hydrochemical information into a mathematical groundwater model for the purpose of source identification and quantification was presented by Gorelick, et al. (1983) and Wagner and Gorelick (1986a & b). They deal with the question of identifying the location and magnitude of pollution sources that might have contributed to the contamination of an aquifer. For this, they utilize a two-dimensional numerical model of solute transport in the aquifer, coupled with various optimization techniques. The method might, in principle, be used for recharge estimation provided one had abundant information about the hydraulic and transport properties of the aquifer.

2. PRINCIPALS OF THE MIXING CELL APPROACH

In this chapter a mathematical model is presented for the estimation of recharge and hydraulic parameters of an aquifer under conditions where the hydraulic and transport characteristics of the aquifer are unknown or poorly known. In the model, the aquifer is divided into cells within which the isotopes and dissolved constituents are assumed to undergo complete mixing. This idea derives from the mixing cell approach of Simpson and co-workers (Simpson, (1975), Simpson and Duckstein, 1976; Campana and Simpson, 1984). This approach had been already used for describing the spatial hydrodynamic behavior of a one dimensional non steady flow. Yurtsever and Payne (1978b & 1985) applied the convolution integral to describe the tritium response function in a simplified lumped parameter multi-cell model. Storage coefficients for each cell, mean travel time and aquifer dispersivity were estimated. Campana and Mahin (1985) used the mixing cell approach to assess mean water age, effective porosity and storage coefficient in a limestone aquifer.

In this approach, mass-balance equations are written for each mixing cell, expressing the conservation of water, isotopes and dissolved chemicals. These equations are solved simultaneously by quadratic programming for the estimation of flow components and aquifer hydraulic parameters in a lumped system. A similar approach was used by Woolhiser et al. (1982) to estimate the inflow rate into a river reach. The latter being analogous to a single cell in our model.

In the approach used here the degree to which individual dissolved constituent may be considered conservative is tested a priori by means of a chemical equilibrium model such as WATEQF (Plummer et al., 1976) or NETPATH ((Plummer et al., 1991) Constituents which do not pass this test are either disregarded or assigned a suitably small weight in the quadratic program.

The model presented below relies basically on three types of conceptual models applied in hydrology (and in hydrodynamics): (a) Evaluation of the motion of water and solutes with a multi-compartmental mixing cell model as suggested by Rasmussen (1982) and Campana and Simpson (1984): (b) solution of a set of water and dissolved constituents mass balance equations via a quadratic programming optimization scheme exemplified by works carried out by Woolhiser, et al. (1982); Adar (1984) and Adar, et al. (1988) and (c) a mathematical model combining an inverse process to estimate compartmental conductances and storage coefficients distribution in a multi-compartmental model for a non-steady flow as described by Adar and Sorek (1989, 1990)

The model is based on accounting for natural available tracers such as dissolved chemicals, stable isotope ratios and electrical conductivity measurements that are relatively easily obtained and measured in an aquifer and in potential recharge sources. It conceptualizes an aquifer that is discretized into finite cells such that the spatial distribution of any aquifer characteristic such as dissolved constituents and hydraulic heads are approximated by unique values for each tracer and head assuming a complete dilution within each cell (the mixing cell principle). The following assumptions are considered to be true in the aquifer:

1. Tracers are conservative: all reactions, dissolution and/or precipitation are negligible. The spatial change in the concentration of the solute is solely due to dilution. In principle, non-conservative tracers can be utilized as long as the rate of change due to subsurface water mineral interaction or rate of decay functions are known.

2. Seasonal pulsation of fluxes for each cell can be represented by mean values spanning over a time interval in which the hydraulic head may be regarded as a constant value or as an average value of cyclic process in time. Pulsation of hydraulic heads throughout observation points in the aquifer may change in amplitude. yet their period phases remain alike.

3. Transport of dissolved constituents are dominated by advection process (i.e. compartmental Peclet number is infinite).

Further practical assumptions are embedded in the model: (a) Concentrations of solutes, which are constant within each cell for specific time step, are measurable and known together with the concentrations of the same tracers in the inflow and outflow components; (b) all of the flows entering or leaving the aquifer system are known qualitatively, yet most of the source-sink and discharge flow components are known quantitatively, including the associated concentration of the dissolved constituents.

Being aware of the fact that in groundwater flow, solutes and isotope concentrations change in space and time, we discretized the aquifer into finite cells assuming that within each cell (for a specific time step) solutes and isotopes are fully mixed, yet their concentrations may differ from one cell to another. Thus, it is justified to assign each cell a mean indicative set of solutes and/or isotopes. With respect to the second assumption one can identify each potential recharge source and represent a potential water source that can contribute to the system via the set of tracers.

3. ASSESSMENT OF GROUNDWATER FLUXES AND RECHARGE COMPONENTS

In this model the aquifer is subdivided into a finite number of discrete cells **N** and time is represented by discrete intervals Δt. Each dissolved constituents is taken to be uniformly distributed within any space-time domain due to complete mixing. Each constituent **k** is taken to be conservative. Seasonal fluctuations in flow rates are smoothed out by considering their temporal integrals over semi-annual cycles. With regard to the above ideas, we will now write a set of balance equations for the flux and solutes within a given time period Δt and for each cell **n** separately.

For a fluid with constant density, the water balance for the **n**-th compartment is expressed by the following equation:

$$Q_n - W_n + \sum_{i=1}^{I_n} q_{in} - \sum_{j=1}^{J_n} q_{nj} = S_n^* \frac{dh_n}{dt} \qquad (1)$$

where **In** and **Jn** denote the number of sources and/or compartments from which flow enters the **n**-th compartment, and leaves it, respectively; q_{in} and q_{nj} denote the fluxes from the **i**-th source or compartment into the **n**-th one, and from the **n**-th one into the **j**-th one, respectively; Q_n and W_n denote the fluid sources (such as point injection) and sinks (such as pumping), respectively; S_n^* represents the storage capacity within cell **n**: and h_n denotes the hydraulic head associated with that compartment. Figure 1 illustrates the aforementioned flow parameters in a schematic compartmental system.

As the head (h_n) for each compartment varies, we may identify points in time, say t_1 and t_2 ($t_2 > t_1$), at which the hydraulic heads are the same (e.g. at the beginning and at the end of a specific season). This means that over that time interval $t=t_2—t_1$ (regardless of the sequence of changes in heads during this time interval), the total magnitude of the derivatives (dh_n/dt) in each compartment has not changed. Hence, since $S_n^* \pi S_n^*(t)$, we obtain:

$$\frac{1}{\tau}\int_{t_1}^{t_2} S_n^* \frac{dh_n}{dt} dt = 0 \quad ; \quad h_{n;t_1} \cong h_{n;t_2} \qquad (2)$$

Thus, by integrating equation (1) over a time period $t=t_2—t_1$ and dividing by t we obtain accordingly:

$$\overline{Q}_n - \overline{W}_n + \sum_{i=1}^{I_n} \overline{q}_{in} - \sum_{j=1}^{J_n} \overline{q}_{nj} = 0 \qquad (3)$$

where all the parameters have the same meaning as in (1), but represent average values over time interval Δt e.g.:

$$\overline{q}_{in} = \frac{1}{\tau} \int_{t_1}^{t_2} q_{in} dt \qquad (4)$$

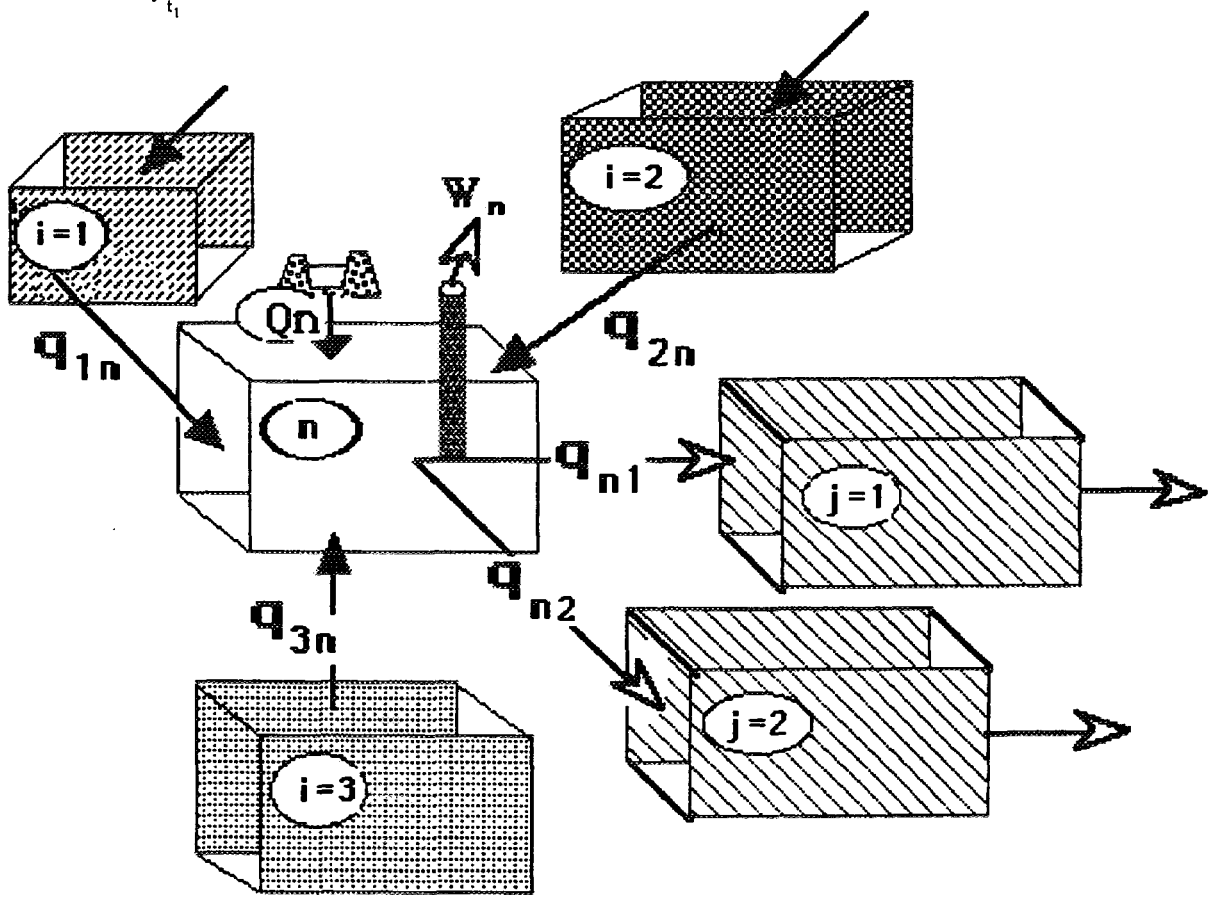

Figure 1. Symbols of designating fluxes, sinks, sources and schematic flow configuration between cells through permeable boundaries.

Note that equation (3) expresses a quasi-steady state situation resulting from the time averaging process.

For quasi-steady state variations of concentrations, when mixing cell concept is applied, and in view of assumption 1 and equation (1c), we write a mass balance expression for a dissolved constituent **k**, in cell **n**.

$$\tilde{C}_{nk}\overline{Q}_n - \overline{C}_{nk}\left[\overline{W}_n + \sum_{j=1}^{J_n} \overline{q}_{nj}\right] + \sum_{i=1}^{I_n} \overline{q}_{in}\overline{C}_{ink} = 0 \quad k=1,2,....,K \qquad (5)$$

where $\bar{C}_{ink}$ is the average concentration of solute **k** entering cell **n** together with the flux coming from cell **I**; $\bar{C}_{nk}$ denotes average concentration of the k^{th} constituent within cell **n** ; and $\tilde{C}_{nk}$ is the average concentration of **k** associated with source Q_n. However, when constructing balance equations from field measurements, equations (3) and (5) should account for various errors. Water balance (equation (3)) may not hold because of an error in identifying and measurements of fluxes or rates of pumpage. Mass balance of solutes (equation (5)) may be affected by analytical errors in measuring concentrations. especially in quantifying cell concentrations. To reflect the above mentioned inconsistencies, we introduce an error term into equation (3) and (5) respectively.

$$\bar{Q}_n - \bar{W}_n + \sum_{i=1}^{I_n} \bar{q}_{in} - \sum_{j=1}^{J_n} \bar{q}_{nj} = e_n \tag{6}$$

$$\tilde{C}_{nk}\bar{Q}_n - \bar{C}_{nk}\left[\bar{W}_n + \sum_{j=1}^{J_n} \bar{q}_{nj}\right] + \sum_{i=1}^{I_n} \bar{q}_{in}\bar{C}_{ink} = e_{nk} \tag{7}$$

where e_n, and e_{nk} are the deviations from flux and solute balance in cell **n**, respectively. Upon combining equations (6) and (7) to a matrix form for each compartment, **n**, we obtain:

$$\underline{\underline{C}}_n q_n + \underline{D} = \underline{E}_n \tag{5}$$

where $\underline{\underline{C}}_n$ is a matrix with known concentrations in cell **n** of the form

$$\underline{\underline{C}}_n = \begin{bmatrix} 1 & ,1 & ,\ldots,1 & ,-1 & ,-1 & ,\ldots,-1 \\ C_{1n1}, & C_{2n1}, & \ldots, C_{I_n n1}, & -C_{n1}, & -C_{n1}, & \ldots, -C_{n1} \\ C_{1n2}, & C_{2n2}, & \ldots, C_{I_n n2}, & -C_{n2}, & -C_{n2}, & \ldots, -C_{n2} \\ . & . & . & . & . & . \\ . & . & . & . & . & . \\ C_{1nK}, & C_{2nK}, & \ldots, C_{I_n nK}, & -C_{nK}, & -C_{nK}, & \ldots, -C_{nK} \end{bmatrix} (K+1)*(In+Jn) \tag{8}$$

where the first row accounts for water balance, and the other **K** rows express solute mass balance where **K** is the total number of tracers used in the analysis. Negative sign denotes coefficients which are associated with outgoing fluxes. $\bar{C}ink$ denotes the concentration of the **k**-th species flowing into cell **n** from cell **i**. $\underline{q}_n$ is a vector of the unknown fluxes through the boundaries of cell **n**, described by:

$$\underline{q}_n = \left[\bar{q}_{1n}, \bar{q}_{2n}, \ldots, \bar{q}_{I_n n}, \bar{q}_{n1}, \bar{q}_{n2}, \ldots, \bar{q}_{nJ_n}\right] (In+Jn)*1. \tag{9}$$

$\underline{D}_n$ is a vector containing elements that are measured and known quantitatively in cell **n** (such as known fluxes of pumpage), described by:

$$\underline{D}_n = \left[\left(\bar{Q}_n - \bar{W}_n\right), \left(\tilde{C}_{n1}\bar{Q}_n - C_{n1}\bar{W}_n\right), \left(\tilde{C}_{n2}\bar{Q}_n - C_{n2}\bar{W}_n\right), \ldots, \left(\tilde{C}_{nK}\bar{Q}_n - C_{nK}\bar{W}_n\right)\right] (K+1)*1 \tag{10}$$

E is the error vector in cell n, described by:

$$\underline{E} = [e_n, e_{n1}, e_{n2}, \ldots, e_{nK}](1+K)*1 \qquad (11)$$

The total flux components in the aquifer can now be estimated by a minimization of the square error sums **J**. Similar to a procedure suggested by Adar (1984), by virtue of equation (5) and by assembling the square error terms over all cells we obtain:

$$J = \sum_{n=1}^{N} \left[\underline{E}_n^T \underline{\underline{W}} \underline{E}_n \right] = \sum_{n=1}^{N} \left[\left(\underline{\underline{C}}_n q_n + \underline{D}_n \right)^T \underline{\underline{W}} \left(\underline{\underline{C}}_n q_n + \underline{D}_n \right) \right] \qquad (12)$$

where $(\ )^T$ denotes transpose and $\underline{\underline{W}}$ represents a diagonal matrix comprised of weighting values about estimated errors (independent of each other) expected for each of the terms building the mass balance for the fluid and the dissolved constituents. The weighting matrix, $\underline{\underline{W}}$ also reflects the degree of confidence to which the tracers are assumed conservative and the degree of accuracy of the chemical and isotope analyses. The solution of equation (12) for $\mathbf{q_n}$ is decomposed into linear and non-linear parts and **J** can be minimized to evaluate $\mathbf{q_n}$ by an algorithm developed, for example, by Wolf (1967)

3.1 MODEL TESTING WITH SYNTHETIC DATA

Test has been made of the mathematical model for which sets of synthetic data have been generated for a hypothetical aquifer divided into mixing cells. The test was conducted to evaluate the ability of the computer code to solve the mathematical model for the unknown fluxes. A schematic representation of the flow regime prevailing during the first test is given in Figure 2.

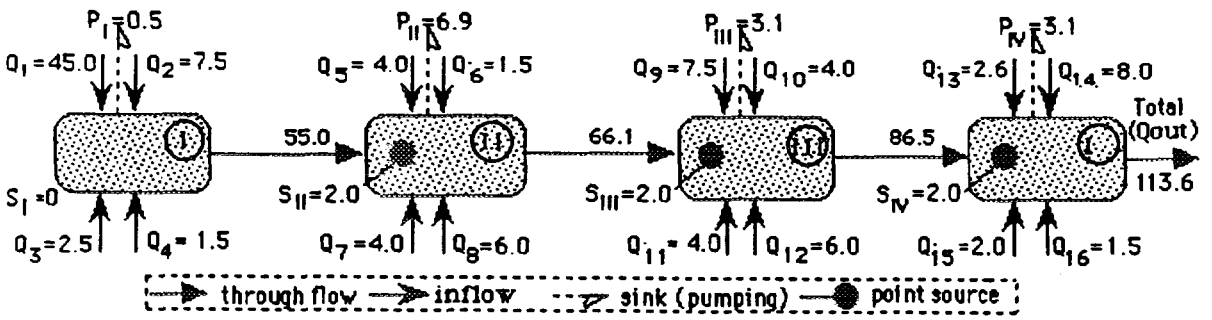

Figure 2: Schematic compartmental aquifer used for testing the mathematical algorithm. Q = rate of inflow (m^3/t); P = rate of discharge (m^3/t).

Recharge into the aquifer derives from nineteen sources. Discharge (**Qout**) occurs at the outlet from cell IV, and via pumpage from each of the four cells. To generate the synthetic data, the corresponding recharge and discharge rates were

assigned arbitrary values (consistent with water balance requirements) in discharge units as indicated in the figure.

In this schematic flow system, the number of unknown flow rates exceeds the number of isotopic and chemical species by 19 to 14. There are four inflows into cell 1 and five into each of cells 2, 3 and 4. One inflow into each of the last tree cells is considered as a point source term (S). The assigned inflows and sources are posted in Figure 2, and the assigned concentrations appear in Table 1. Inflows Q_4, S_{II}, S_{III} and Q_{16} have identical isotopes and chemical signatures. Q_4 and Q_{16} could represent, for example recharge from floods, and so have inflows Q_8, Q_{12}, and Q_{15} which could represent, for example stream bed infiltration due to perennial effluent. S_{II} and S_{III} might designate a common point source such as leakage from surface water tank. The sink terms (such as pumpage) are 0.5, 6.9, 3.1 and 3.1 (volumetric flux units) for cells I, II, III and IV, respectively.

Table 1. Synthetic concentrations used in Test 1.

inflow	EC[a]	Mg	Ca	Na	K	HCO_3	Cl	NO_3	SO_4	F	Li	Si	D[b]	18_O[c]
1	353.8	0.74	1.97	0.97	0.062	3.08	0.205	0.082	0.42	0.023	0.0026	18.01	-73.8	-9.73
2	187.1	0.36	0.81	0.39	0.035	0.89	0.093	0.001	0.80	0.001	0.0003	18.18	-66.3	-8.56
3	146.0	0.53	1.13	0.51	0.049	1.40	0.081	0.035	0.66	0.006	0.0012	17.53	-60.6	-8.55
4	332.3	0.62	2.31	0.69	0.174	2.97	0.151	0.030	0.38	0.025	0.0013	16.83	-58.7	-7.41
5	304.5	0.10	0.24	2.01	0.048	2.52	0.263	0.022	0.05	0.036	0.0022	14.00	-67.2	-8.70
6	370.3	0.77	1.67	1.70	0.069	3.04	0.690	0.224	0.14	0.008	0.0032	8.80	-63.1	-6.52
7	454.0	1.28	2.52	0.98	0.028	3.71	0.419	0.059	0.64	0.012	0.0016	16.35	-76.3	-10.18
8	242.0	0.39	1.51	0.33	0.063	1.20	0.086	0.044	0.63	0.030	0.0020	17.70	-67.1	-8.98
source	332.3	0.62	2.31	0.69	0.174	2.97	0.151	0.030	0.38	0.025	0.0013	16.83	-58.7	-7.41
9	356.0	1.72	3.18	0.73	0.034	3.64	0.140	0.046	1.93	0.015	0.0016	14.80	-67.0	-8.43
10	147.8	0.84	0.41	0.33	0.030	0.07	0.070	0.008	0.98	0.120	0.002	7.80	-68.9	-9.36
11	362.0	0.66	2.06	0.87	0.050	2.93	0.140	0.080	0.51	0.022	0.0023	17.10	-69.3	-9.66
12	242.0	0.39	1.51	0.33	0.063	1.20	0.086	0.044	0.63	0.030	0.0020	17.70	-67.1	-8.98
source	332.3	0.62	2.31	0.69	0.174	2.97	0.151	0.030	0.38	0.025	0.0013	16.83	-58.7	-7.41
13	355.5	0.70	2.10	0.89	0.050	2.90	0.175	0.142	0.56	0.024	0.0023	18.55	-72.3	-9.68
14	444.2	1.15	3.21	0.76	0.029	3.39	0.275	0.027	1.36	0.052	0.0016	14.58	-68.6	-9.56
15	242.0	0.39	1.51	0.33	0.063	1.20	0.086	0.044	0.63	0.030	0.0020	17.70	-67.1	-8.98
16	332.3	0.62	2.31	0.69	0.174	2.97	0.151	0.030	0.38	0.025	0.0013	16.83	-67.7	-9.70
source	302.8	0.05	0.30	2.89	0.020	2.52	0.320	0.021	0.19	0.080	0.0037	14.25	-74.8	-9.44
Cell 1	321.9	0.677	1.788	0.865	0.0608	2.712	0.1832	0.0678	0.480	0.0194	0.0022	17.98	-71.32	-9.461
Cell 2	322.9	0.655	1.733	0.902	0.06	2.646	0.2019	0.065	0.468	0.0207	0.0021	17.44	-70.89	-9.303
Cell 3	314.4	0.734	1.807	0.818	0.060	2.538	0.1793	0.0594	0.623	0.0254	0.0020	16.78	-69.885	-9.136
Cell 4	324.2	0.744	1.895	0.844	0.0583	2.593	0.1871	0.0575	0.657	0.0286	0.0020	16.62	-69.856	-9.235

Concentrations in meq l^{-1} unless otherwise indicated.
a-μMHOcm^{-1}
b- Deuterium (0/00)
c- Oxygen-18 (0/00)

These values, while arbitrarily chosen (so as to maintain isotopic and chemical balance for each species, are nevertheless in accord with actual data from the Aravaipa Valley in southern Arizona to be later presented in the field application section. With the assigned flow rates and concentrations, the error terms in equations. (6) and (7) should be zero, and the minimization of **J.** in equation (12) should yield a zero value for the optimum **J.**

For the purpose of our exercise, we treated the discharge, Q_{out}, and pumpage rates, P_1- P_4, as known terms, and the recharge rates, Q_1-Q_{19}, as unknowns. To facilitate convergence of the quadratic program we followed the approach of Woolhiser, et al. (1982) setting the components of the diagonal weight matrix W_n, corresponding to each cell n equal to:

$$Wn_{11} = Q_{0ut}^{-2} \quad ; \quad Wn_{1=k,1+k} = C_{ok}^{-2} \quad ; \qquad k=1,2,3,...,K \tag{13}$$

where C_{ok} is the concentration of the k^{th} species at the outlet from the aquifer. The effect of this weighting scheme is to normalize the balance equations so they are all expressed on a scale relative to the downstream outflow equations.

Table 2 compares the calculated and assigned inflow rates, and Table 3 juxtaposes the calculated and assigned mass flow rates for the isotopic and chemical species. Again, the results are seen to be very good, the total water balance and the total isotopic and chemical balance errors are negligible, and attributed to the computer round off procedure.

Table 2. Comparison between assigned and calculated inflows obtained with exact data.

Inflow	Q_1	Q_2	Q_3	Q_4	Q_5	Q_6	Q_7	Q_8	Q_9	Q_{10}	Q_{11}	Q_{12}	Q_{13}	Q_{14}	Q_{15}	Q_{16}	TOTAL
Assigned inflows (m^3/t)	45.00	7.50	2.50	1.50	4.00	1.50	4.00	6.00	7.50	4.00	4.00	6.00	2.60	8.00	2.00	1.50	113.60
Calculated inflows (m^3/t)	44.30	7.40	2.36	1.44	4.17	1.56	4.37	6.30	7.58	3.97	3.76	6.04	2.68	8.07	2.08	1.54	113.59

Flow between cells	I to II	II to III	III to IV
Assigned flow)m^3/t)	55.0	66.1	86.5
Calculated flow (m^3/t)	55.368	66.372	86.396

m^3/t - cubic meters per unit time

The computed flow rates in Table 2 are seen to be very close to the true (assigned) values. Q_4, and Q_{16}, or Q_8, Q_{12}, and Q_{15} derived from the same source (carry same isotopic and chemical signature) but contributing to two separate cells, are correctly identified. The errors in Tables 2 and 3 stem essentially from rounding off and incomplete convergence of the Wolf algorithm. Indeed, experience has shown, that for the same test case, these small deviations vary with the type of computer system. Other tests with different cell and flow configurations are reported in Adar (1984) and Adar et al. (1988).

The tests show that, as long as the input data are precise including a proper aquifer discretization into mixing cells, the algorithm is able to estimate correctly fluxes of recharge and subsurface flow components. It is important to note that within a particular cell, each potential flow component must have a unique chemical and isotopic values. The same source, however, may contribute to

several cells. The number of computed fluxes (unknowns) may be less or more than the number of isotopic and chemical species entering into the model. The number of mass balance expressions, however, should exceed by far the number of unknowns.

Table 3. Comparison between assigned and calculated mass flow rates obtained with exact data.

Ionic and isotopic species	True mass flow	Estimated mass flow	Percentage error
EC*	36,815.94	36,788.62	0.074
Mg	1,019.42	1,019.21	0.021
Ca	4,289.66	4,285.13	0.106
Na	2,211.36	2,211.69	-0.015
K	260.52	260.18	0.130
HCO_3	17,984.83	17,987.77	0.016
Cl	756.67	756.13	0.074
NO_3	406.21	408.85	0.651
SO_4	3,570.12	3,562.35	0.218
F	60.55	60.41	0.228
Li	1.61	1.58	0.749
Si	1,894.77	1,894.87	-0.005
^2H	-7,942.92	-7,943.85	-0.012
^{18}O	-1,049.62	-1,049.50	-0.009
Total	325,133.7	325,326.6	0.060

* Electrical conductivity.

3.2 FIELD APPLICATIONS

The above-mentioned model has been implemented to assess the rate of recharge and groundwater fluxes in two arid basins: the Aravaipa basin in Arizona, USA, and in the Arava Valley shared by Israel and Jordan. In these basins, a simple longitudinal aquifer is recharged through mountain front alluvial fans. Other sources of recharge to be considered are temporal erratic floods and upward leakage from deep semi-confined aquifers.

3.2.1 ARAVAIPA BASIN, ARIZONA, U.S.A.

The Aravaipa Valley is located in the eastern Sonora desert in Arizona, USA (Fig 3). The valley is surrounded by the Galiuro volcanics (a sequence of andesitic and rhyolitic tuffs and lava) on the west, and the Santa Teresa granitic pluton, and the Pinaleno granodioritic pluton from the eastern boundary of the valley.

The Aravaipa Valley is a narrow graben filled with fluvial sediment interbedded with thin lake deposits. The main water course is the ephemeral Aravaipa Creek that becomes perennial at the Aravaipa Springs at the head of the Aravaipa Canyon. Annual precipitation from large winter storms and high intensity convective summer storms range from 355 mm in the lower valley, to 430 mm in the upper valley, and to 510 mm in the surrounding mountains (For further geologic and geophysical information, the reader is referred to Adar, 1984).

Three hydrological units were identified in the Aravaipa watershed: a mountain aquifer and two alluvial aquifers, separated by lacustrine clay layers. The lower alluvial unit is formed mainly by the older alluvium. It is confined from above by low permeability layers which are continuous across the width of the valley except for the western pediments. This suggests that this unit may be recharged directly from the eastern mountains and by infiltrating rainfall and runoff from the alluvial pediments. The main source of water in the valley is the upper water table unit. This aquifer is limited to the course of the Aravaipa Creek and to the alluvial fans of the confluences with major tributaries. This aquifer is 20 kilometers long and is generally narrow ("1,000 m), except near major alluvial fans where its width may exceed 1,500-2,000 m.

In general, available hydrological information for the valley is very poor and consists of an approximated depth of wells, a few driller's logs and two transmissivity values for the upper and confined aquifers respectively. Discharge from the lower confined aquifer by livestock and irrigation wells is estimated at 62,000 m3/year. Discharge from the water table aquifer by domestic use and irrigation wells is estimated at 2.96×10^6 m3/year; and discharge from the valley through the Aravaipa spring is estimated at 1.22×10^7 m3/year. Twenty five years of records regarding the hydrological activities of the valley suggest that it is in a steady state (Arad and Adar, 1981).

Chemistry and environmental isotopes are used to identify potential sources of recharge and possible mixing and dilution of waters from different sources. For this we make use of the fact that water that infiltrates to a depth at which evaporation ceases usually maintains constant ^{18}O and D ratios, unless mixing or dilution with waters having different isotopic compositions takes place.

One hundred and sixty two water samples from 109 well sites, springs and stream gages (including floods) were analyzed for major cations (including Li), anions (including F), Si, TDI, electrical conductivity and temperature. Water from 74 sites were analyzed for Oxygen-18 and 47 of the latter sites were checked for deuterium (D) values. The upper and lower aquifers exhibit different ranges for temperature, water level and ratios of environmental isotopes. Higher temperatures and heavier stable isotopes are found throughout the entire area of the lower aquifer.

Higher piezometric heads in the lower confined unit is a clear indication that water may leak upward from the confined aquifer along the entire valley, through electrical conductivity and temperature logs throughout the confining layer were not sensitive enough to indicate the presence of such leaking. The

hydraulic connection between the two aquifers has been implied on the basis of Tritium and Carbon-14 variations during a pumping test, and by the relationship between Tritium (H-3) and C-14 ratios. (Adar & Neuman, 1986, 1988).

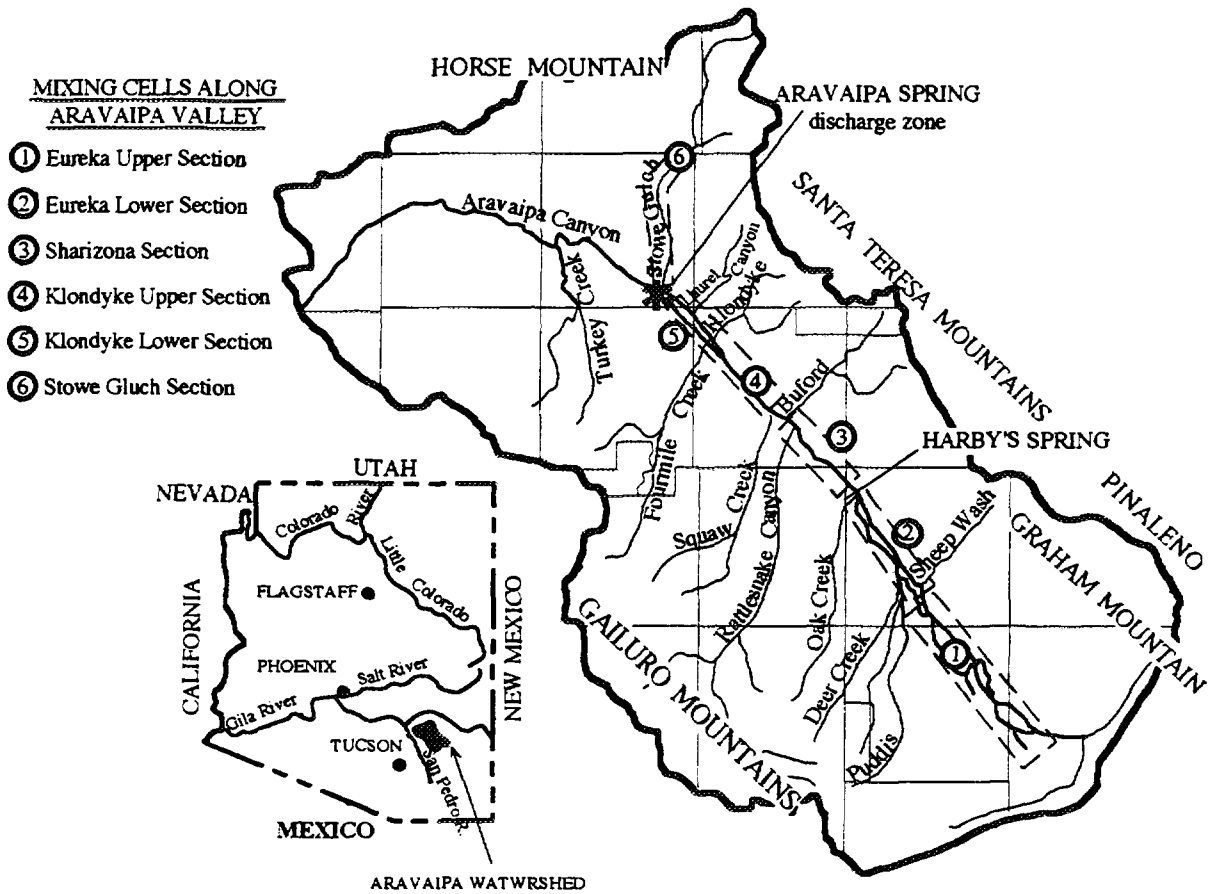

Figure 3: Aravaipa Valley, Arizona, USA.

Most of the mountain springs in the basin have a low discharge rate and present a different dissolved chemical content. It suggests that the mountain springs drain small local aquifers within high fractured zones. Based on the local geology it is possible that these small aquifers, which are in direct contact with the alluvial units, recharge the valley aquifers. Although the mountains on both sides of the valley are at almost the same elevation, the isotopic ratio of the collected rainfall was found to be extremely different (Adar and Long, 1987). Furthermore significant different in geology and type of mineralogy have been observed along the mountains surrounding the valley. The aforementioned

differences between the mountain aquifers can be used in the above-mentioned model to elaborate on the relative quantities that recharge the alluvial aquifers.

Aquifer Division into Mixing Cells

The modeling area is subdivided into five mixing cells as marked in Figure 3. The chemical concentration assigned to each cell are taken to be the average of values determined in wells, tapping the unconfined aquifer within the confines of the suggested cell. In general, multi-variables cluster analysis may provide the tool for aquifer partitioning as long as the group division makes sense regarding the geographic and hydrogeologic distribution. As an added check on the manner in which the water samples were grouped into representative cell values, we used activity diagrams as exemplified via the WATEQF computer program (Truesdel and Jones, 1973, Plummer et al., 1976).

The division of the upper aquifer into cells and the considered flow components are illustrated in Figure 4. The major components of potential sources of recharge into the water table aquifer are: (1) intermittent stream recharge along Aravaipa Creek during and after winter and summer floods; (2) inflows through the alluvial fans at the confluences with major mountain washes; (3) lateral inflows through the upper layers of the Old Alluvium, and (4) upward leakage from the deep aquifer (**ul** in Fig. 4). Rates of known fluxes at the Aravaipa Springs (**Qout**) and known rates of pumping (**P**) from each cell, are also given in Figure 4. In this model, recharge due to direct infiltration of rainfall is disregarded due to: (1) the limited outcrops of the alluvial aquifer; (2) an arid climate with extremely high temperature, and (3) the depth of the water table. This recharge component is deemed to be insignificant. To include it formally in our model would require sampling of infiltrating rain water below the root zone within which major chemical changes are expected. This was beyond the scope of our research.

A complete description of chemical and isotopic characteristics associated with each cell and with outflows and potential inflow components is given in Adar and Neuman, 1988. The data were used to establish the known matrix of concentrations - matrix **C** (equation 4). The unknown flow component **q** were obtained by minimizing J (equation 12) via quadratic programming utilizing Wolf algorithm (1967).

The weight matrix **W** (equation 13) is taken to be diagonal and the non-zero terms are assigned in the following manner: $W_{ll} = Q_{out}^{-2}$ and $W_{ll} = w_k^{-2}(C_{ok}\beta_k)^{-2}$ where l=k+1; k=1,2,3,...,k. Here **Qout** and **Cok** are known rate of outflow from the downstream cell and the concentration of the k^{th} species at the Aravaipa Spring respectively. β_k is the coefficient of variation in determining the laboratory standards and w_k is a coefficient varying between 0 and 1 describing the conservancy level of the k^{th} species. Actual values used for β and ω_κ for various species are given in Chapter 6 (Table 8). The balance equation are normalize so that they are all expressed on a scale relative to the outflow at

Aravaipa Spring. Furthermore, the effect of dividing by βk^2 is to reduce the weight of the k^{th} constituent in proportion to measured laboratory errors.

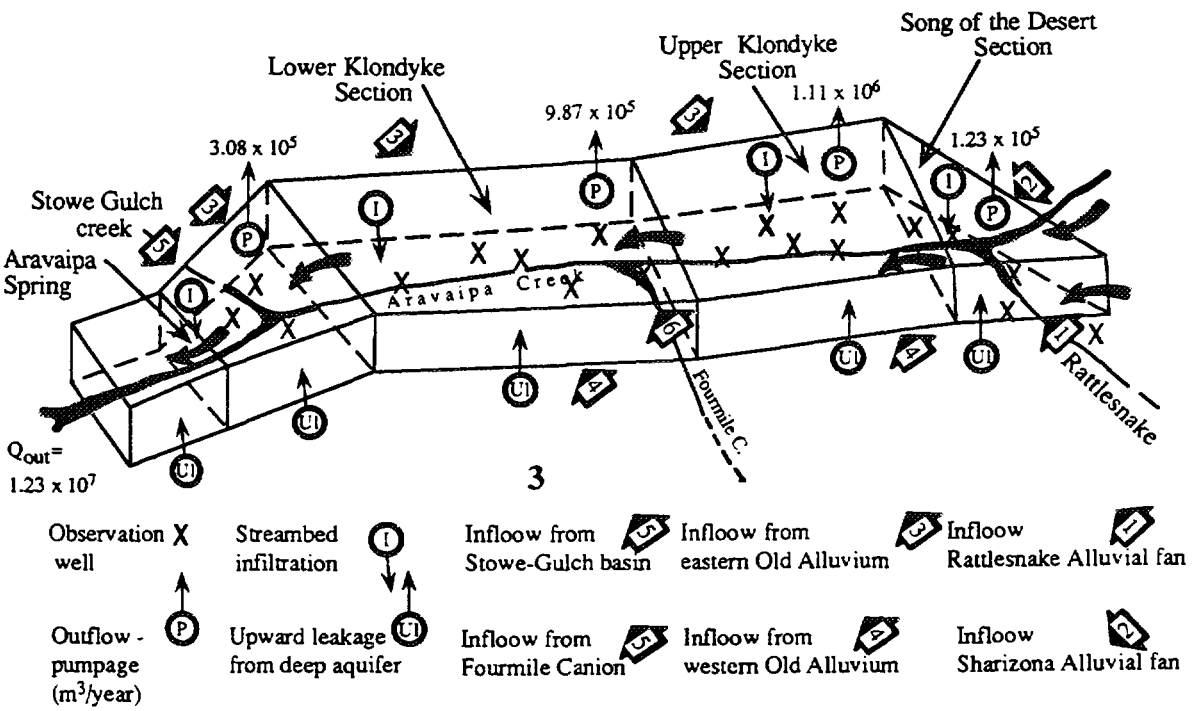

Figure 4: Outline of the modeled portion of the water table aquifer in the Aravaipa Valley

The total number of unknown flow rates in the model, including flow rates in-between the cells, is 23. For each cell there is a water balance and 14 chemical and isotopic balance expressions, resulting in a total of 75 equation. The most probable result with the lowest water and salt balance deviations is given in Table 4.

The results as presented in Table 4 reveal the following findings about recharge in the lower portion of the Aravaipa Valley:

1. Most of the lateral (mountain front) recharge derives from the eastern pediments. The western pediments probably recharge mainly the lower aquifer.
2. Stream bed infiltration contributes about 4% of the total recharge per year. This can be explained in the light of the short length and duration of floods in Aravaipa Creek.
3. Among all the alluvial fans, Stowe-Gulch seems to provide most of the inflow, almost 46% of the total recharge.
4. In the absence of significant pumpage from the lower confined aquifer, the only major avenue of discharge from the deep aquifer is by upward leakage. This flow component provides an important source of fresh water for the upper aquifer.

Table 4: Computed inflow rates into the water table aquifer

Cell No.	Source		Rate of inflow as percent of the total recharge
1	Inflow from	upper valley	3.606
		alluvial fans	0.213
		winter floods	0.000
		summer floods	0.000
		eastern pediments	0.893
		upward leakage	0.020
2	Inflow from	western pediments	7.738
		eastern pediments	4.362
		winter floods	0.030
		summer floods	2.131
		upward leakage	3.908
3	Inflow from	alluvial fans	0.684
		eastern pediments	7.526
		western pediments	1.022
		winter floods	0.000
		summer floods	0.748
4	Inflow from	Stowe-Gulch Basin	46.332
		upward leakage	14.640
		winter floods	0.000
		summer floods	0.000
5		upward leakage	2.333
Water balance			-3.808
Salt balance			+0.310

Although detailed sensitivity analysis of the model to errors in data and to the weight parameters is not presented in this chapter, results must be interpreted with caution. For further descriptions of results the reader is referred to Adar and Nueman, 1988. Nevertheless, the model appears to be a useful to extract and support subsurface flow and recharge information.

3.2.2 ARAVA VALLEY, NEGEV DESERT, ISRAEL & JORDAN

The southern Arava valley is a narrow down faulted rift valley, about 16 km. wide and extending about 80 km. north to the Gulf of Eilat. It is an extremely arid

basin with average annual precipitation of about 50 mm. Due to its geological and geophysical nature, the rift forms a low base level into which surface, as well as subsurface, flows drain from the surrounding mountains. In the valley, water were found in (a) sandstone of Paleozoic age, (b) sandstone of Lower Cretaceous, (c) limestone of Cretaceous age, and (d) alluvial fill of Quaternary age. Figure 5 illustrates the geography, various geological outcrops and location of well fields along the valley. Due to extremely complex hydrogeologic structures caused by

tilted faults followed by upward and/or downward movement of blocks, it was almost impossible to obtain detailed and reliable information on the physical properties of each structural component of the aquifer system. Therefore a quantitative assessment of the flow system including the sources of recharge by numerical modeling is not possible at this stage.

Groundwater of varying chemical and isotopic qualities are exploited by wells drilled in the valley and along its margins. Wells drilled into different blocks and layers and springs showed that due to differences in lithology and mineralogy, each source of recharge provides the alluvial aquifer with water of a specific chemical composition. Also, the isotopic ratios of oxygen-18 to oxygen-16, and deuterium to hydrogen are determined by the geographic location, including prevailing temperatures and the altitude of the area in which recharge occurs. The spatial isotopic and ionic distribution within the alluvial aquifer along the Southern Arava Valley seems to be affected mainly by the relative proportion of recharge contribution from each source. Hence, dilution and mixing are assumed to be the major mechanisms which control the hydrochemical and isotopic composition of the alluvial groundwater reservoir.

The temporal distribution of dissolved ions have revealed almost constant concentrations over the last twelve years. Furthermore, the piezometric head distribution and the pumping regime also seem to be constant for that period. Hence, changes in heads and concentrations of most species within cell $\mathbf{n}$ during time interval $\Delta \mathbf{t}$ turned out to be very small and thus negligible for modeling purposes. This implies an almost steady state hydrological flow regime, at least for the past decade. For further hydrogeological description and for the detailed flow pattern, as suggested by the environmental tracer's distribution the reader is referred to Rosenthal et al., (1990).

Six ions, TDI, deuterium (D) and oxygen-18 (^{18}O) parameters were used in a multi-variable cluster analyses to isolated and characterize 12 major potential sources of recharge and to divide the alluvial aquifer into 6 homogeneous compartments (Adar et al. 1992). Several close configurations of cells and potential inflows were modeled. For only four close configurations, the Wolf Algorithm solver provided a solution. For the remainder, unbounded or no solutions were obtained. A comprehensive description of the quantitative assessment of subsurface fluxes within the southern Arava basin is given in Adar et al. (1992).

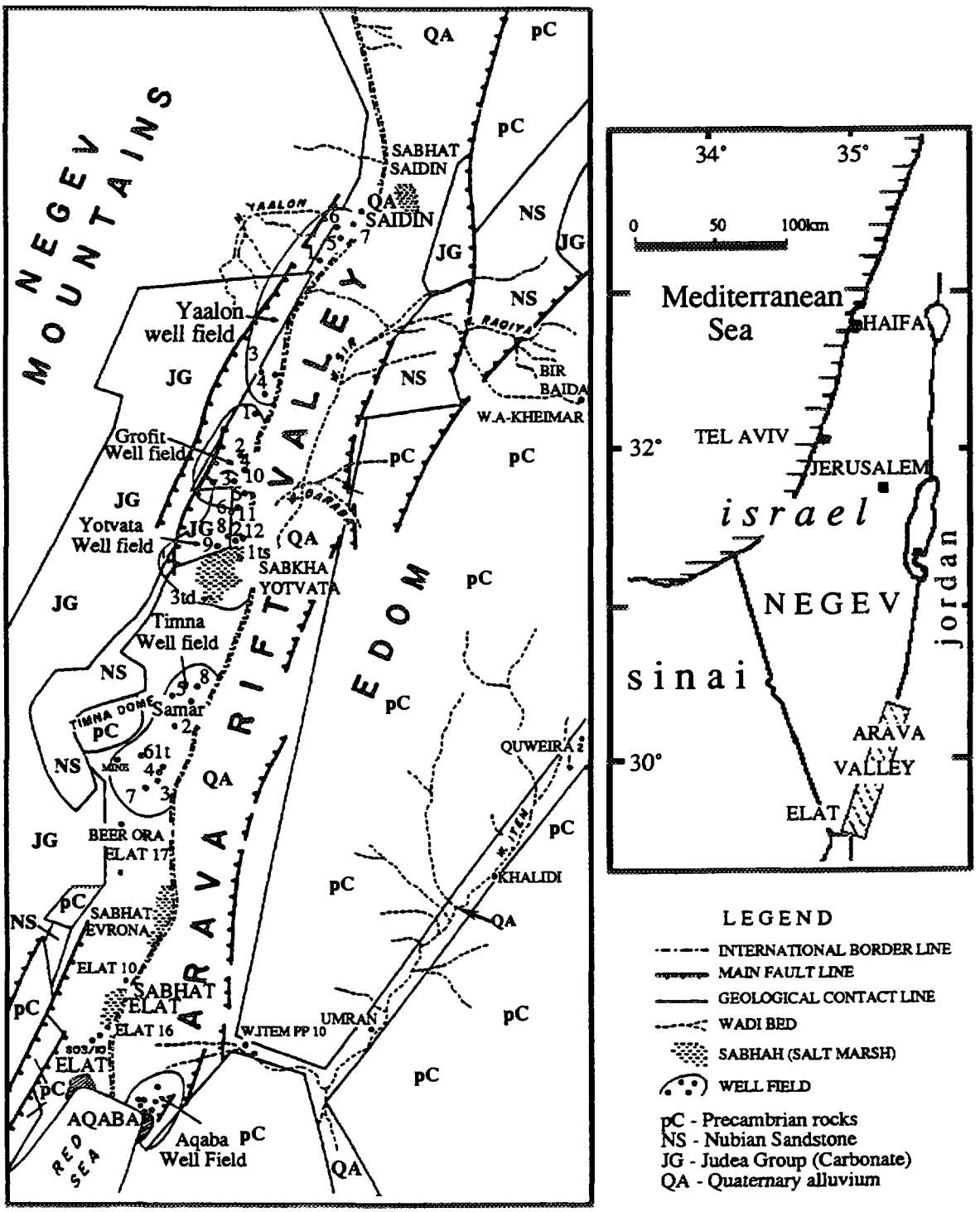

Figure 5: A map of southern Arava basin showing the location of main well fields and a schematic appearance of major geological units.

Figure 6 presents the results for 12 potential inflows obtained with 7 dissolved ions and 2 isotopes. Subsurface recharge components and internal fluxes are given in 10^6 m^3/year. The errors associated with the optimization of mass balance equations of dissolved ions varies from 0.45% to 6.85%. It is important to notice, however, that the calculated fluxes are heavily dependent upon the rates assigned to the known outflows. The absolute values of these deviations have no real meaning aside from the fact that for more reliable flow configurations, one may expect to obtain lower deviations. As a result of the model, for the first time, a quantitative estimation of the contribution from the Nubian sandstone aquifer is obtained. Also, the significant contribution from the mountain - front recharge to the alluvial aquifer is clearly demonstrated.

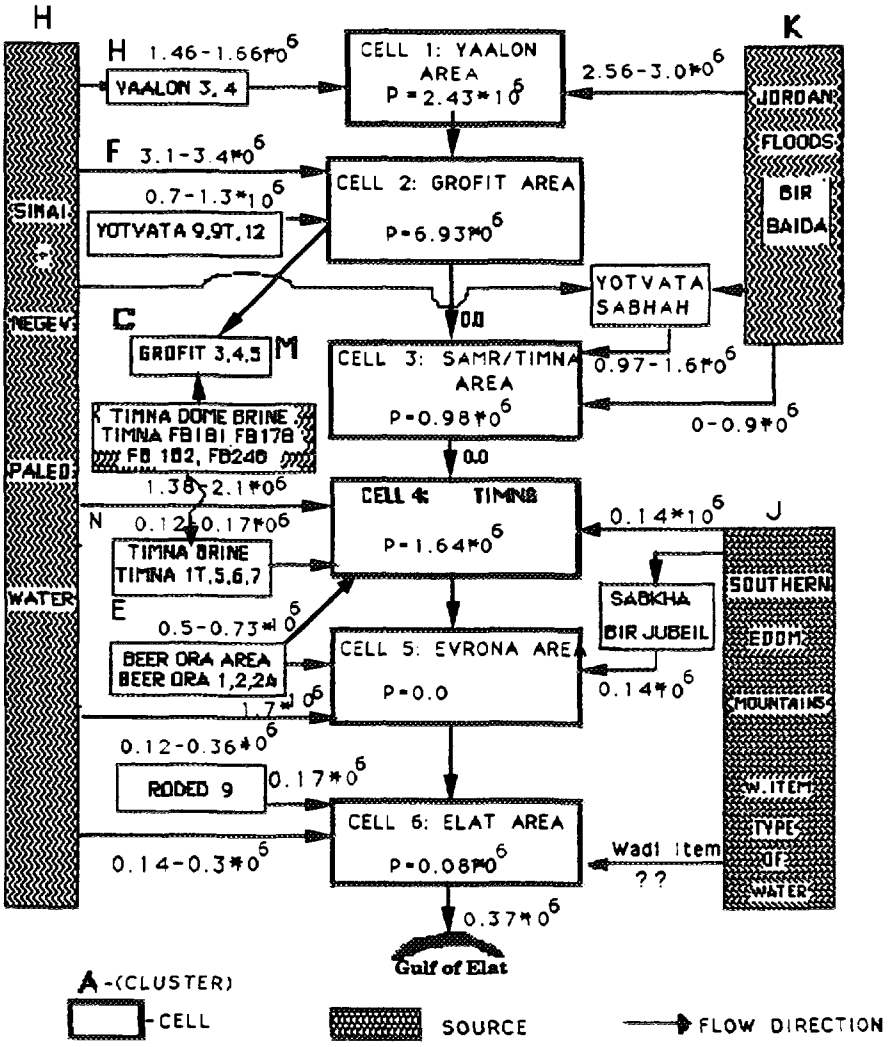

Figure 6: Calculated fluxes and recharge components in the Southern Arava valley.

4. ESTIMATION OF TRANSMISSIVITIES ACROSS FLOWING BOUNDARIES

The solved time averaged fluxes are now used to estimate conductances through cell's boundaries. Conductance is defined as the ability of an active boundary to transmit a unit flux per unit head gradient across the boundary. It can be related to transmissivity as further be discussed below. The flux through a common permeable boundary, is proportional to the hydraulic head difference across this boundary. Integrating Darcy's linear momentum expression for any time interval over a control volume surrounding such a boundary for inflow from cell **i** into cell **n**, yields:

$$\bar{q}_{in} = T^{*}_{in}\left(\bar{h}_i - \bar{h}_n\right) \tag{14}$$

where T_{ij}^{*} (= T_{ji}^{*}) denotes conductance at the common boundary between cells i and **j**, and $\bar{h}$ denotes the time average of measured hydraulic head. Similarly, the outflow from cell **n** to cell j, reads

$$\bar{q}_{nj} = T^{*}_{nj}\left(\bar{h}_n - \bar{h}_j\right) \tag{15}$$

Writing equations (14) and (15) for all permeable boundaries of the multi-compartmental system, we obtain a global set of the form:

$$\underline{q} = \underline{\underline{h}}\,\underline{T}^{*} \tag{16}$$

where $\underline{\underline{h}}$ is a diagonal matrix of hydraulic head differences given by:

$$h_{\xi\eta} = \delta_{\xi\eta}\left(\bar{h}_i - \bar{h}_j\right) \quad ; \quad \xi,\eta = 1,2,3,\ldots,N_b \tag{17}$$

and $\underline{q}$ denotes the vector of solved averaged fluxes across permeable boundaries, given by:

$$q = \left[\, \bar{q}_1, \bar{q}_2, \bar{q}_3, \ldots, \bar{q}_{N_b} \,\right]_{N_b * 1} \tag{18}$$

Here, N_b denotes the number of permeable boundaries in the aquifer cell system. δ_{xh} is the Kronecker delta, where **x=h** for permeable (active) boundary. $(h_i - h_j)$ represents the averaged head difference governing outflow from cell i into cell **j**. The vector of conductances. $\underline{T}^{*}$, is given by:

$$\underline{T}^{*} = \left[T_1^{*}, T_2^{*}, T_3^{*}, \ldots, T_{N_b}^{*}\right]_{N_b * 1} \tag{19}$$

Hence, conductances in the aquifer cell system $\underline{T}^{*}$, are solved using the set of equations as described in equation (16).

In a compartmental simulation of an aquifer, conductances coefficient T^* replaces transmissivity term T used in a continuum approach. In view of equation (14), e.g. for inflow boundaries, we may write the relation between T^* and T in the following form:

$$\bar{q}_{in} = T^*_{in}\left(\bar{h}_i - \bar{h}_n\right) = T_{in} b_{in} \frac{\bar{h}_i - \bar{h}_n}{l_{in}} \qquad (20)$$

where T_{in} denotes the transmissivity between observation wells **i** and **n**, which represent the characteristic properties of the respective cells (the mixing cell approach). b_{in} denotes the length of the (**in**) boundary between those cells and l_{in} represents the distance between observation wells **i** and **n**, normal to the boundary (**in**) as depicted in Figure 7.

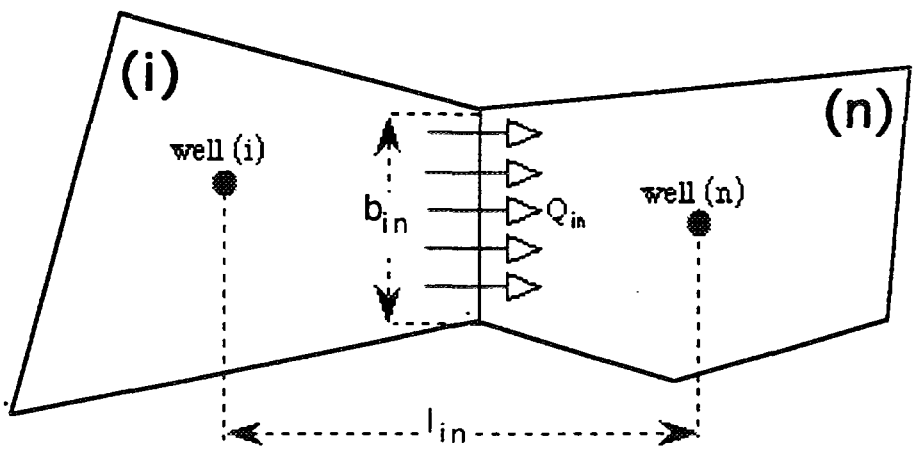

Figure 7. Scheme of flow between two compartments (i) and (n) and illustration of the l_{in} and b_{in} dimensions.

4.1 TESTING THE MODEL WITH SYNTHETIC DATA

The conceptual model and the computer code were tested with a set of synthetic data which was generated for a hypothetical aquifer divided into mixing cells. The test was conducted to evaluate the ability of the computer code to solve the mathematical model for unknown fluxes and transmissivities simultaneously. The test was conducted with four cells. The set up of the cell's configuration and the assigned fluxes, sinks, sources (volume per unit time), and transmissivities (area per unit time) for the internal boundaries are given in Figure 8. Not as in the previous test, a multi-flow cell configuration was assigned for testing the algorithm and the computer code. Cell **I** has a sink (pumping) term and receives four inflows through external boundaries without a source term. Fluxes leaving cell **I** contribute water to cells **II** and **III** [36 and 20 (l^3/t), respectively]. Cell **II** also receives water from four external sources and has both sink and source terms (No. 9 in Fig. 8). Subsurface fluxes leave cell **II** and flow

into cells III [5(l^3/t)] and IV [45(l^3/t)]. Cell III has three external sources with a sink term and water leaves this cell only into cell IV [40(l^3/t)]. Cell IV has two sources with a sink term. The total subsurface outflow is 100 (l^3/t). Two sources contribute the same type of water to more than one cell. Sources #13 and #16 are the same and recharge cells X and XII, respectively. Sources #10, # 14 and #15 are also the same and contribute the same type of water to cells IX, XI and XII, respectively. All together seventeen unknown external sources. The total number of unknowns is 37 (17 external inflows, 15 internal fluxes and 15 transmissivities). Some of the cells: VI, VII, VIII, X, XI and XII were also assigned sink (pumping rates) terms. The numbers in the ellipsoids designate rates of inflows (recharge) from external sources.

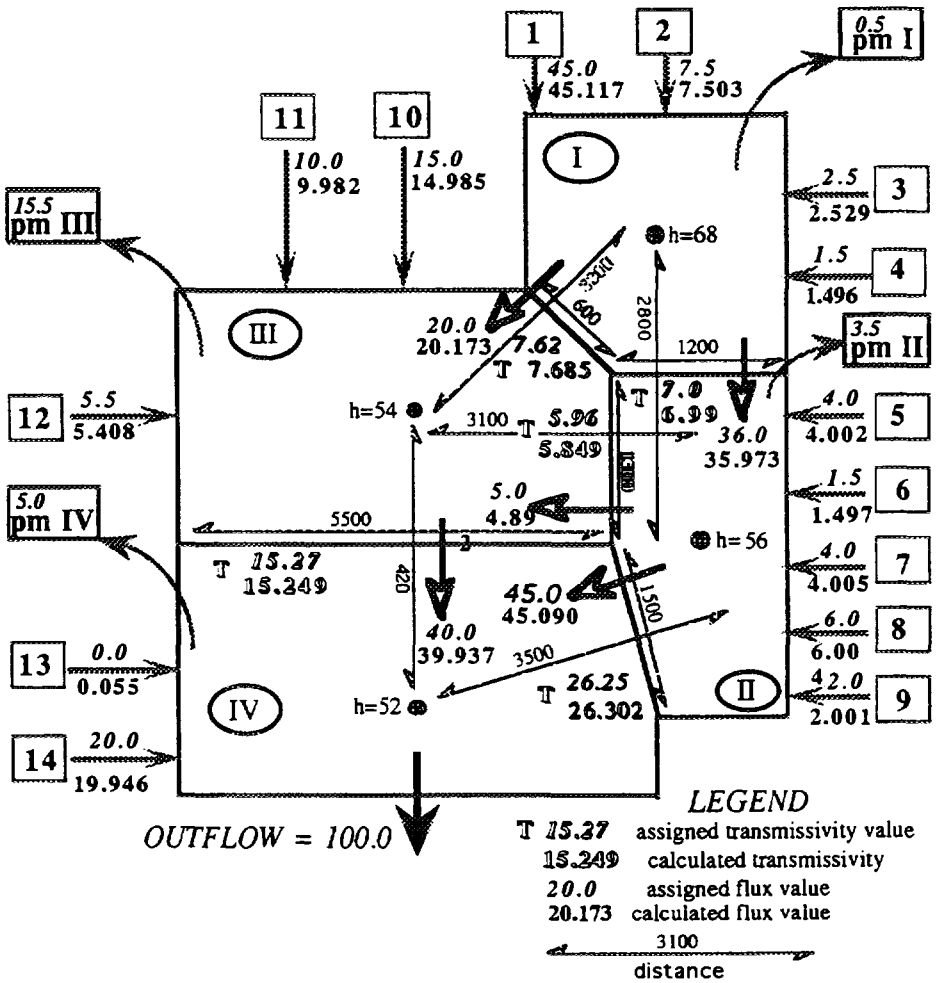

Fig. 8 Schematic compartmental aquifer used for testing the mathematical algorithm. P_m = rate of discharge (in volume per unit time).

To test the ability of the model to evaluate transmissivities across active boundaries, equations (14) and (15) were embedded in equations (6) and (7). The transmissivities then can be calculated using Darcy's type of equation as given in Equation (20). So far, to solve for the time - averaged fluxes, the only data that was required aside from the qualitative knowledge of the flow system were the

spatial distribution of environmental tracers. However, for the calculation of transmissivities, one should add the distribution of hydraulic heads as well as the dimensions of the cells; mainly the size of active boundaries. The combination between head distribution and cell geometry suggests which of the boundaries is active and require evaluation of the transmissivities. All the above-mentioned dimensions are also posted in Figure 8.

In Figure 8 the upper numbers designate the assigned fluxes or transmissivities and the lower numbers are the results obtained from the model. The assigned fluxes were used to calculate the tracers' concentrations for every cell, an information which was later used as known or "measured" data for testing the algorithm. As expected for synthetic data and zero error terms in the water and mass balance equations, the calculated transmissivities and fluxes are almost identical. The negligible differences may attributed to the numerical round off errors. The test show that, as long as the input data are precise including a proper aquifer discretization into mixing cells, the algorithm is able to estimate correctly transmissivities, fluxes of recharge and subsurface flow components.

4.2 FIELD APPLICATION: DISTRIBUTION OF TRANSMISSIVITIES IN THE SOUTHERN ARAVA VALLEY.

The same mixing cell configuration as obtained by the multi variable cluster analysis (Figure 6), and the data set of the dissolved minerals and isotopes were used to assess the spatial distribution of transmissivities over the southern Arava valley. Hydraulic heads were assigned to imaginary wells located at the center of each cell by interpolation from piezometric maps. Additional information on cell's geometry, in particular, the width of the boundaries and the length between the wells, was estimated from topographic maps. A new set of water and chemical (including isotopes) mass balance expressions (equations 6 & 7) were introduced into the mathematical algorithm, such that the flux terms q_{in} & q_{nj} were replaced by conductance terms as defined in equations 14 and 15 respectively. Then, transmissivities were estimated using equation (20).

Figure 9 presents the range of results obtained by a simultaneous optimization for transmissivities and components of recharge (inflows). The range of calculated transmissivities and fluxes is a result of modifications made in flow configurations and in cell geometry.

The concentrations and the hydraulic heads which represent each compartment are assigned to the geometric center of the cell. In other words, an imaginary well is posted at the geometric center of a cluster of observation holes presenting a similar type of water. Therefore, the actual location of boundaries between cells is not known precisely. In fact, the most one can say is that the boundary should be somewhere between the closest extreme well of the nearby cluster forming each cell.

Table 5. Calculated versus measured transmissivities in three sections along the southern Arava Valley (m^2/day).

Section		Measured	Calculated
Yaalon-Grofit area.			**997-1016**
	Ketora 4 (DD)*	1849	
	" (R)**	1209	
	Yotvata 2 (R)	2665	
	" 2 (IT8)***	1400	
	Yotvata11 (DD)	980	
	" 11 (DD	1000	
	" 11 (R)	1060	
	Yotvata12 (R)	2010	
Samar-Timna area			**104-350**
	Samar 2 (?)	400	
	Timna 4 (R)	370	
	Timna FC(IT?)	807	
	Timna 4 (IT3)	4600	
	" (IT1)	2800	
Eilat area			**284-345**
	Eilat 10 (R)	496	
	Eilat m.s. (R)	105	
	Eilat 16 (R)	273	

Since the location of the representative imaginary wells is assigned arbitrarily to the geometric center of the well's cluster (not to the center of the entire cell's area), the exact location of the cells boundaries has no effect on the distance l_{in} between the centers of cells. However, the position of the boundaries, which are always normal to the flow trajectory, affects the width b_{in} of permeable boundaries. The width of the boundaries in the southern Arava Valley were assigned according to the contact between the alluvium and the surrounding hills, as determined from maps and air photos.

Transmissivity values that were obtained by various types of pumping tests in key wells along the valley are listed in Table 5. For most cases, each method provided a different transmissivity. Furthermore, recovery tests with different orientations also revealed different results, which probably reflects the non homogeneity of the aquifer across very short distances. The transmissivity values assessed by the above-mentioned model (also listed in Table 5) are in fairly good agreement with the values found from the pumping tests. It is important to notice, however, that this model allows the evaluation of transmissivities for segments of aquifer with active steady fluxes. For cells with heavy rates of pumping, as in the central section of the `Southern Arava basin, transmissivities can not be evaluated since the inter-cell fluxes are zero. Therefore, it is necessary

to assess simultaneously both transmissivities and fluxes. Similar to the results obtained with the inverse numerical solution, the calculated transmissivities are average values between the nodes. In a compartmental scheme, the values are an assortment of conductances across permeable boundary between cells. In other words, it describes the ability of the boundary to transmit a certain volume of water per unit length of the boundary per unit time.

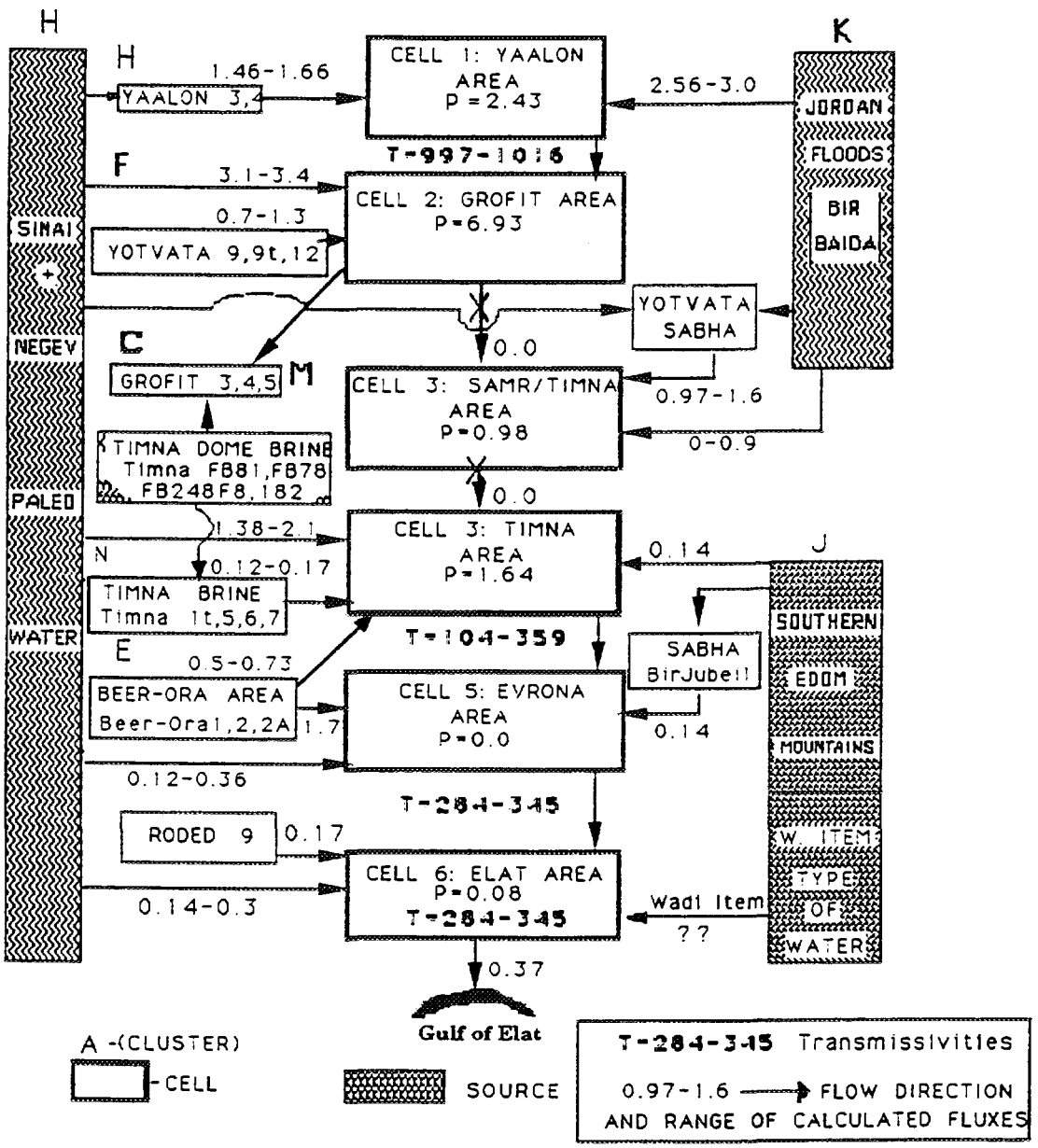

Fig. 9 A schematic flow pattern for the southern Arava Valley with computed transmissivities (in m^2/day) and fluxes (in 10^6 m^3/year).

5. ESTIMATION OF AQUIFER STORAGE COEFFICIENTS

Thus far, fluxes and conductances have been evaluated based on time average compartmental heads and concentrations obtained for time interval Δt. Estimated transmissivities for every active boundary can then be calculated by equation (20).

For the assessment of compartmental storage coefficients, one may use the information about temporary head variations in the flow domain during (or within) the time period Δt (Adar and Sorek, 1989). Suppose one assigns **M** specific observations for compartmental head $h_n^{(m)}$ during time period Δt; (m = 1, 2, ...,M) where $h_n^{(m)}$ denotes the head in cell **n** at time **m** as illustrated in Figure 10.

In view of equations (14) and (15), one may write the temporal values of boundary inflow ($q_{in}^{(m)}$) and outflow ($q_{nj}^{(m)}$) fluxes for each time observation **m** in the following manner:

$$q_{in}^{(m)} = T_{in}^{*}\left(h_i^{(m)} - h_n^{(m)}\right) \tag{21}$$

and

$$q_{nj}^{(m)} = T_{nj}^{*}\left(h_n^{(m)} - h_j^{(m)}\right) \tag{22}$$

In the above equations T_{nj}^{*} is already a known parameter since conductances were already solved. Substituting equations (21) & (22) into equation (1) and assembling for all **N** aquifer compartments, one obtains a global set of linear ordinary equations at time observation **m** of the form

$$\underline{\underline{S}}^{*}\frac{d\underline{h}^{(m)}}{dt} + \underline{\underline{T}}^{*}\underline{h}^{(m)} = \underline{R}^{(m)} \tag{23}$$

where $\underline{\underline{S}}^{*}$ denotes a diagonal matrix of compartmental storage capacity coefficients; $\underline{\underline{T}}^{*}$ denotes the matrix of conductances in which the two terms T_{in}^{*}, and T_{nj}^{*} are associated with permeable boundaries (inflow and outflow respectively). No-flow boundary is expressed by zero term; $\underline{h}^{(m)}$ is a vector of compartmental head terms measured at time observation **m**; and $\underline{R}^{(m)}=(\underline{Q}^{(m)}-\underline{W}^{(m)})$ is a vector of the known compartmental sources (inflows) and sink flux terms.

The goal is to solve for the S_n^{*} storage capacities, for each compartment **n** in the aquifer, given that $h_n^{(m)}$, $R_n^{(m)}$ and T_{in}^{*} (or T_{nj}^{*}) values are known. To do that we rewrite equation (23) to the form:

$$\underline{\underline{X}}^{(m)}\underline{S}^{*} = \underline{Y}^{(m)} \tag{24}$$

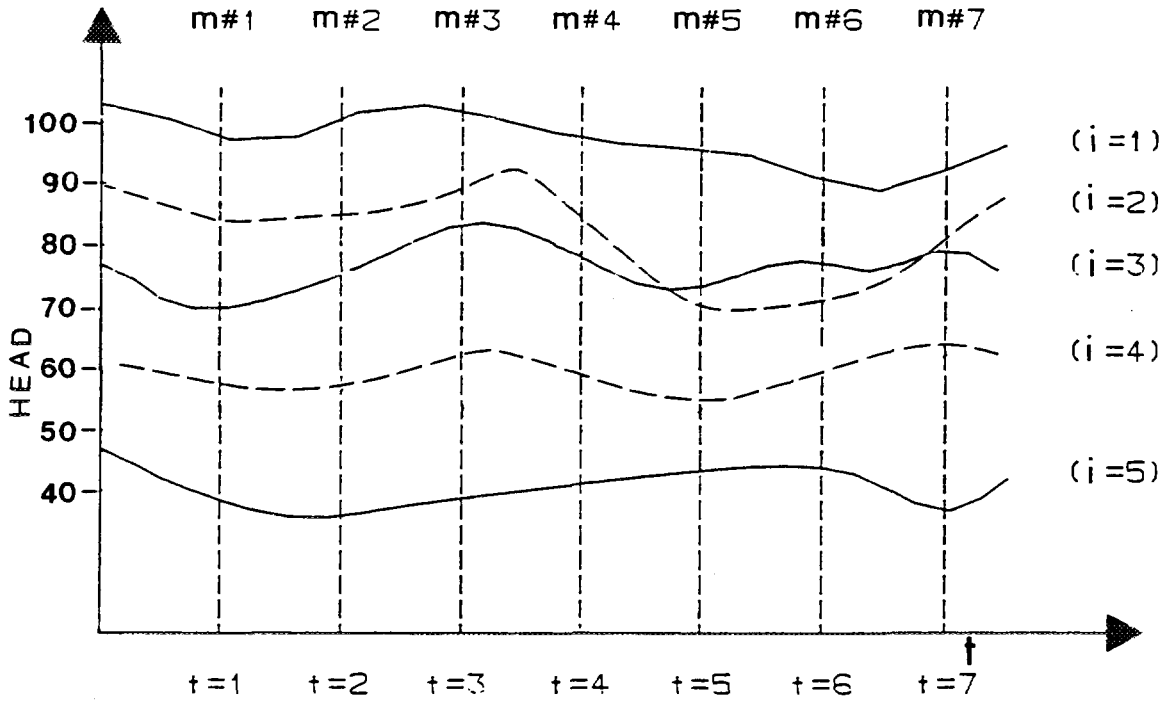

Figure 10 Change of hydraulic head **h** in cells: i=1, i=2, i=3, i=4, and i=5 as function of discrete time observations **m**: t_1 to t_7

where $\underline{\underline{X}}^{(m)}$ is a diagonal matrix of known head rates for all aquifer compartments at time observation **m**

$$X_{ij}^{(m)} = \delta_{ij} \frac{dh_{ij}^{(m)}}{dt} \quad ; \quad i,j = 1,2,3,\ldots,N \tag{25}$$

$\underline{Y}^{(m)}$ is a vector of known terms at observation time **(m)**.

$$\underline{Y}(m) = \left[\underline{R}^{(m)} - \underline{\underline{T}}^{*}\underline{h}^{(m)}\right]_{N*1} \tag{26}$$

and $\underline{S}^{*}$ is the vector of unknown storage capacities for all **n** compartments at observation **(m)**.

$$\underline{S}^{*} = \left[S_1^{*}, S_2^{*}, S_3^{*}, \ldots\ldots, S_N^{*}\right]_{N*1}. \tag{27}$$

Next, upon implementing the Gauss-Markov method (Bard, 1974) for equation (24) through all **M** time observations, we obtain an optimal solution for $\underline{S}^{*}$, of the form

$$\underline{\underline{S}}^{*} = \left[\underline{\underline{X}}^{T}\underline{\underline{X}}\right]^{-1}\underline{\underline{X}}^{T}\underline{Y} \tag{28}$$

where

$$\underline{\underline{X}} = \begin{bmatrix} \underline{\underline{X}}^{(1)} \\ \underline{\underline{X}}^{(2)} \\ \underline{\underline{X}}^{(3)} \\ . \\ . \\ \underline{\underline{X}}^{(M)} \end{bmatrix}_{(N*M)*N} \tag{29}$$

$$\underline{Y} = \left[\left(\underline{R}^{(1)} - \underline{\underline{T}}^{*}\underline{h}^{(1)}\right), \left(\underline{R}^{(2)} - \underline{\underline{T}}^{*}\underline{h}^{(2)}\right), \ldots, \left(\underline{R}^{(M)} - \underline{\underline{T}}^{*}\underline{h}^{(M)}\right)\right]_{(N*M)*1}. \tag{30}$$

Since $\underline{\underline{X}}^{(m)}$ is a diagonal matrix, we can write an explicit expression for S_n^* commencing from equation (28).

$$S_n^{*} = \frac{\sum_{m=1}^{M} \frac{dh_n^{(m)}}{dt}\left[R_n^{(m)} - \sum_{\eta=1}^{N} T_{n\eta}^{*} h_{\eta}^{(m)}\right]}{\sum_{m=1}^{M}\left[\frac{dh_n^{(m)}}{dt}\right]^2} \tag{31}$$

where **h=1, 2,..., N** denotes numbers of active boundaries.

The $h_n^{(m)}$ and $dh_n^{(m)}/dt$ values are at discrete time observations (**m=1,2,...,M**) for each cell **n**.

Compartmental storage capacity S_n^* is related to the storativity S_{sn} or to specific yield S_{yn} for confined and water table aquifers, respectively, by the following expressions

$$S_n^{*} = \phi_n V_n S_{sn} \tag{32}$$

and

$$S_n^{*} = A_n S_{y_n} \tag{33}$$

where A_n is the area of cell **n**, V_n is its saturated volume, and ϕ_n, is the porosity.

5.1 ASSESSMENT OF TRANSMISSIVITIES AND STORAGE COEFFICIENTS FOR OSCILLATING PIEZOMETRIC HEADS

The next test (Test 2) of the mathematical algorithm and the computer code was performed for calculating transmissivities and storage coefficients in an aquifer with periodic distribution of hydraulic heads. It was performed on the same layout of the flow system (16 unknown external fluxes and 16 transmissivities, 3 sources and 4 sink terms) as illustrated in Figure 2. In this test, instead of using a given average head for each of the relevant cells, a temporal distribution of heads is given for each cell and across every active boundary. The time-head distribution was created arbitrarily, i.e. utilizing a sinusoidal function around an average value $\mathbf{h_{av}}$:

$$h(t) = h_{av} + \alpha \sin\left(\frac{2\pi t}{M}\right) \tag{34}$$

where α is the allowed amplitude and **M** is the total number of observations. Twelve head values were assigned for each cell, but not necessarily at the same time observation. Figure 11 shows an arbitrary periodic distribution of hydraulic heads across sixteen active boundaries in four cells. Later in the program, a spline method for curve fitting was used to obtain a polynomial expression describing the time-head distribution in each cell. These expressions were then integrated and the average heads were obtained from the quotients of the integrals over the head distributions and the length of the time intervals. These polynomial expressions were then used to obtain **M=12** synchronized tabulated piezometric heads. Next, upon implementing the **Gauss-Markov** algorithm (equations (28) to (31)) through all **M** observations of heads, an optimal solution for the storage coefficients S^* was obtained.

The implementation of the Gauss-Markov method through all M observations in equation (31) for the four (n=4) system cells resulted in the following storage coefficients for each cell (Table 6):

Table 6. Estimated storage coefficients for each cell in Figure 2.

$S_I^* = 1.1799$	$S_{II}^* = 34.5764$	$S_{III}^* = 5.6183$	$S_{IV}^* = 1.4791$

The relations between S^* to S_S or S_y are given in equations (32) and (33), respectively. Specific storage and/or specific yield can be estimated providing that the porosity and either the volume or the area of the saturated layer are available for confined or phreatic aquifers respectively. The large value of S_2^* emerges from the fact that a relatively large rate of pumping (sink term, Table 6) was assigned to Cell **II**, where also the inflows are very low relative to the other system cells.

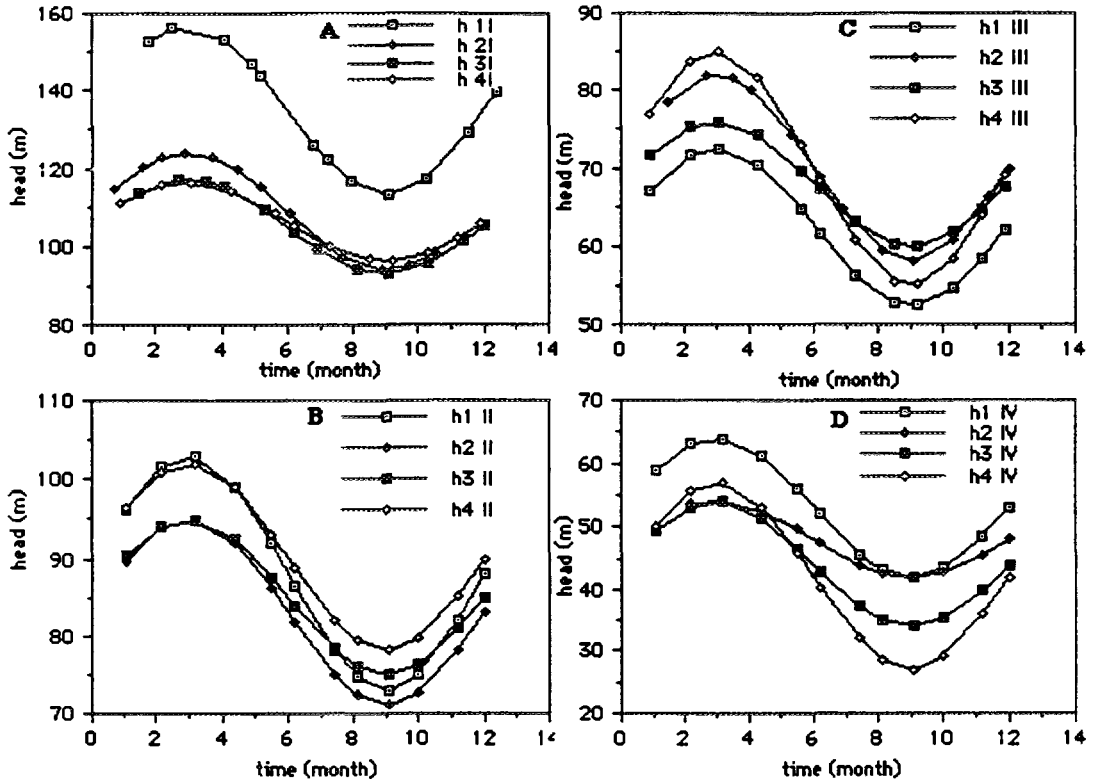

Figure 11: Arbitrary periodic distribution of hydraulic heads across active boundaries in Test 2.

Table 7 shows the results of estimated transmissivities across internal and external boundaries for an oscillating piezometric head regime and for a specific geometry of cells. The test shows that, as long as the data are precise and the number of mass-balance expressions exceeds the number of unknowns, the proposed algorithm is able to estimate correctly transmissivities and storage coefficients across permeable boundaries.

Table 7: Estimated transmissivity values between cells and across external flow boundaries.

Flow From Cell	to Cell	Distance Between Centers (m)	Width of Boundary (m)	Calculated Head Differences (m	Calculated Transmissivities (m^2/t)	Estimated Transmissivities (m^2/t)
I	II	1000.0	255.0	19.9	10.98	10.916
II	III	1500.0	385.0	19.9	12.97	12.983
III	IV	750.0	410.0	20.0	7.96	7.883

Table 7: Continued
Estimated transmissivity values between cells and across external flow boundaries.

Cell	Number of Active Boundaries	Distance Between Centers (m)	Width of Boundary (m)	Head Difference (m)	Calculated Transmissivities (m^2/t)	Estimated Transmissivities (m^2/t)
I	1	2000.0	375.0	35.0	6.86	6.792
I	2	1500.0	625.0	8.7	2.00	2.029
I	3	1750.0	250.0	5.1	3.50	3.418
I	4	2350.0	200.0	6.4	2.80	2.689
II	5	3300.0	330.0	8.1	5.00	4.898
II	6	2800.0	800.0	3.2	1.75	1.588
II	7	900.0	180.0	5.0	4.00	4.288
II	8	1200.0	360.0	10.2	2.00	1.972
III	9	1550.0	750.0	2.5	6.20	6.382
III	10	2250.0	300.0	9.9	3.00	3.020
III	11	1750.0	175.0	8.0	5.00	4.628
III	12	3000.0	360.0	9.8	5.00	4.800
IV	13	4200.0	480.0	13.1	1.75	1.856
IV	14	3600.0	1200.0	8.2	3.00	2.984
IV	15	1800.0	600.0	4.1	1.50	1.565
IV	16	4000.0	600.0	2.1	5.00	5.051

6. SENSITIVITY ANALYSIS: EFFECT OF ERRORS IN THE DATA

In real field situations the input data associated with each cell such as concentrations, piezometric head, and the dimensions of the flowing boundaries, are not known with the appropriate precision. Also, it might be that not all sources of recharge and the flow components have been properly identified. Therefore, the basic assumptions behind the model are not fully satisfied. To examine the effect of erroneous input data on the quality of such estimates, a schematic flow pattern for a simple longitudinal flow system, as illustrated in Figure 12, is repeatedly solved after corrupting the synthetic input data with various levels of non correlated Gaussian noise.

The rationale for the particular method used to generate our noise stems from the assumption that laboratory errors are a major cause of error in isotopic and hydrochemical analysis. The first step was to generate normal errors of zero mean and unit variance $N_{(0,1)}$ by means of the formula (Box and Muller, 1958, as cited in Bard, 1974):

$$N_{(0,1)} = (-2 \log_{10} U_1)^{0.5} \cos(2\pi U_2) \qquad (35)$$

where $\mathbf{U_1}$ and $\mathbf{U_2}$ are independent random variables drawn from uniform distribution. Next, each "true" $\mathbf{C_k}$ value entering into the model was transformed into a noisy concentration $\mathbf{C_k^*}$ according to:

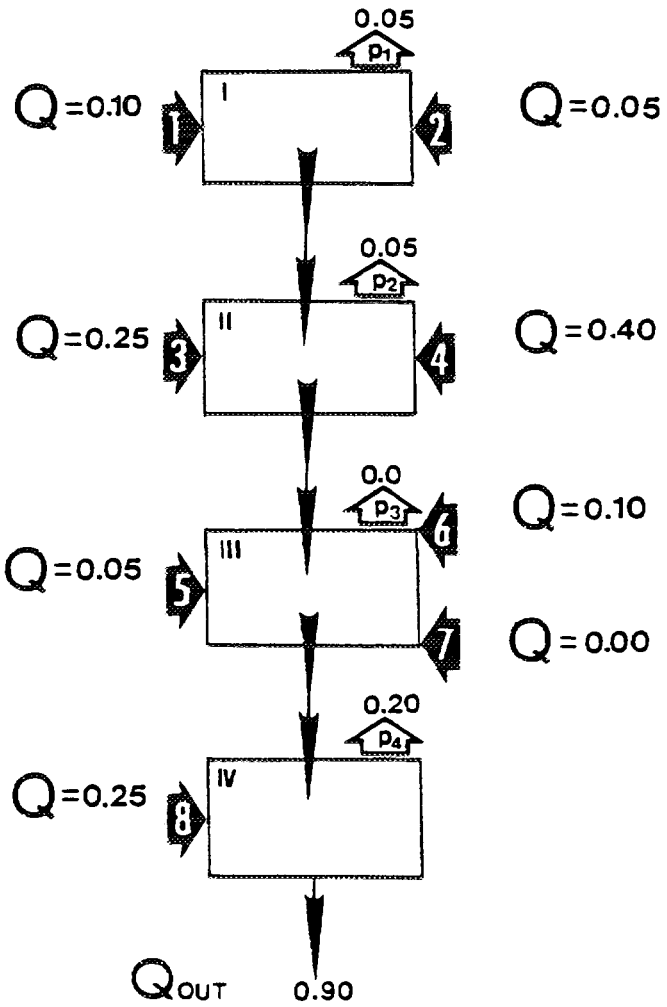

Figure 12: Schematic flow configuration used for sensitivity analyses
Q - rate of inflow; P - rate of pumping or discharge (Vol./time)

$$C_k^* = C_k\left[1+\beta_k N_{(0,1)}\right] \tag{36}$$

where β_k is a weighting parameter controlling the magnitude of the corrupted concentration C_k^* relative to that of the "true" concentration C_k. This causes the error to increase linearly with concentration, which seems to be realistic for laboratory data. When the noise was made independent of concentration, the Wolf algorithm at times failed to converge. In the case of a single river reach, Woolhiser, et al. (1982), found that errors in C are more important than errors in sink or sources when the number of flow rate equations in the model is less than the number of chemical balance equations.

A test was conducted with 100 noisy C data sets for β value equals to 0.05. In this particular test, only concentrations of the dissolved constituents were perturbed as being the most sensitive parameters to laboratory and field analyses. Results are illustrated in Figure 13 A. The Monte Carlo simulation was performed with perturbed concentrations restricted to an ionic balance of 4 %, electrical conductivity (**EC**) to **TDI** ratios between 35 and 55, and D to ^{18}O ratios between 6.5 and 8.5. For each appropriately perturbed set of data, the quadratic program was used to obtain an estimate of the unknown **Q** values. Figure 13A reveals that the mean **Q** values converge to stable values after about 20-40 realizations. Adar et al. 1988 found that it converged almost at the same level regardless of the magnitude of β, but within the framework of the above-mentioned constraints. However, the magnitudes of the estimated average fluxes (**Q**) depend heavily on the magnitude of β. When β = 0.2, these averages (with the exception of Q_7 which is zero) differ from the true values of 30-140%. When β = 0.01, this difference is reduced to 0.2-4%. Though the larger β is, the greater the error of estimation, the rate at which the estimation error increases with β, is decreased as the amplitude of the noise goes up.

Table 8. Statistics and Coefficient of conservancy w_k for 14 isotopic and ionic species from repeated laboratory standards (Analytical Laboratory, University of Arizona, 1984).

Species	Expected value	No. of repeated analyses	Average μ	Standard deviation σ	Coefficient of variation $\sigma / \bar{\mu}$	w_k
EC**	420.0	150	422.0	13.99	0.0316	0.90
Mg	56.5	17	57.6	3.13	0.0543	0.70
Ca	141.0	20	136.3	14.09	0.1030	0.60
Na	207.0	27	202.7	20.84	0.1030	0.60
K					0.0540*	0.45
HCO_3	724.0	27	761.5	87.53	0.1150	0.30
Cl	251.0	30	229.9	37.86	0.1650	1.00
NO_3	558.0	30	573.3	76.32	0.1330	0.10
SO_4	223.0	29	232.2	14.23	0.0613	0.30
F					0.0900*	0.20
Li					0.0600*	0.20
Si					0.1500*	0.20
^2H	-58.0	122	-58.1	3.71	0.0639	1.00
^{18}O	-8.6	78	-8.56	0.198	0.0230	1.00

* Estimated values obtained from UOA Analytical Center, Tucson, Ariz.
** Electrical conductivity.

A second test was performed in which different β_k values were assigned to the various isotopic and chemical species k according to:

$$\beta_k = \frac{\sigma_k}{\mu_k}. \tag{37}$$

Here μ_k is the mean of a large number of concentrations determined for laboratory standards of the **k** species, and σ_k is the associated standard deviation as given in Table 8. In this manner β_k becomes the coefficient of variation of the error in determining the laboratory standard for the **k** species. Two hundred and fifty realizations were performed to examine the stability and the rate of convergence of the calculated fluxes. Results are illustrated in Figure 13B. Results indicate that in spite of the general increase in the magnitude of β (Table 8), the system remains stable though it seems to converge after 40 to 80 realizations with greater deviations from the "true" assigned values.

The stricter the constraints, the closer is the average **Q** to the true flow rates. Adar et al. (1988) found that for data perturbed far beyond the aforementioned constraints, the solver failed to converge, reaching an unbounded solution. In fact, results of chemical composition from analytical laboratories are always checked for maintaining ionic balance. The same data is also examined for the linear correlation between EC and TDS. Similarly, a local constant slope is known to exist between deuterium and oxygen - 18. Detailed results for other combinations of constraints are given in Adar (1984), and the importance of ion balance for a single cell model was demonstrated for laboratory mixtures by Woolhiser, et al. (1985).

7. SUMMARY

This study demonstrates the use of hydrochemistry and environmental isotopes in an arid basin, such as the Aravaipa Valley and the southern Arava basin, where information about hydraulic gradients and aquifer parameters is relatively limited. The available data do not allow one to compute recharge from above, vertical leakage between aquifers, lateral recharge from tributaries or recharge from the surrounding mountain aquifers. This mathematical model can extract quantitative hydraulic information from spatial distribution of dissolved chemicals and stable isotopes. The latter information is often more easily accessible. The proposed model computes these flow components (and others) on the basis of the known or estimated total outflow from the basin and on the basis that the dissolved ions and environmental isotopes can be obtained for all outflows and potential inflow components. A qualitative assessment of the spatial distribution of potential recharge sources, sinks and local sources, and the subsurface flow pattern must be known. These data were obtained qualitatively on the basis of all the available geologic, hydrologic, and hydrochemical information.

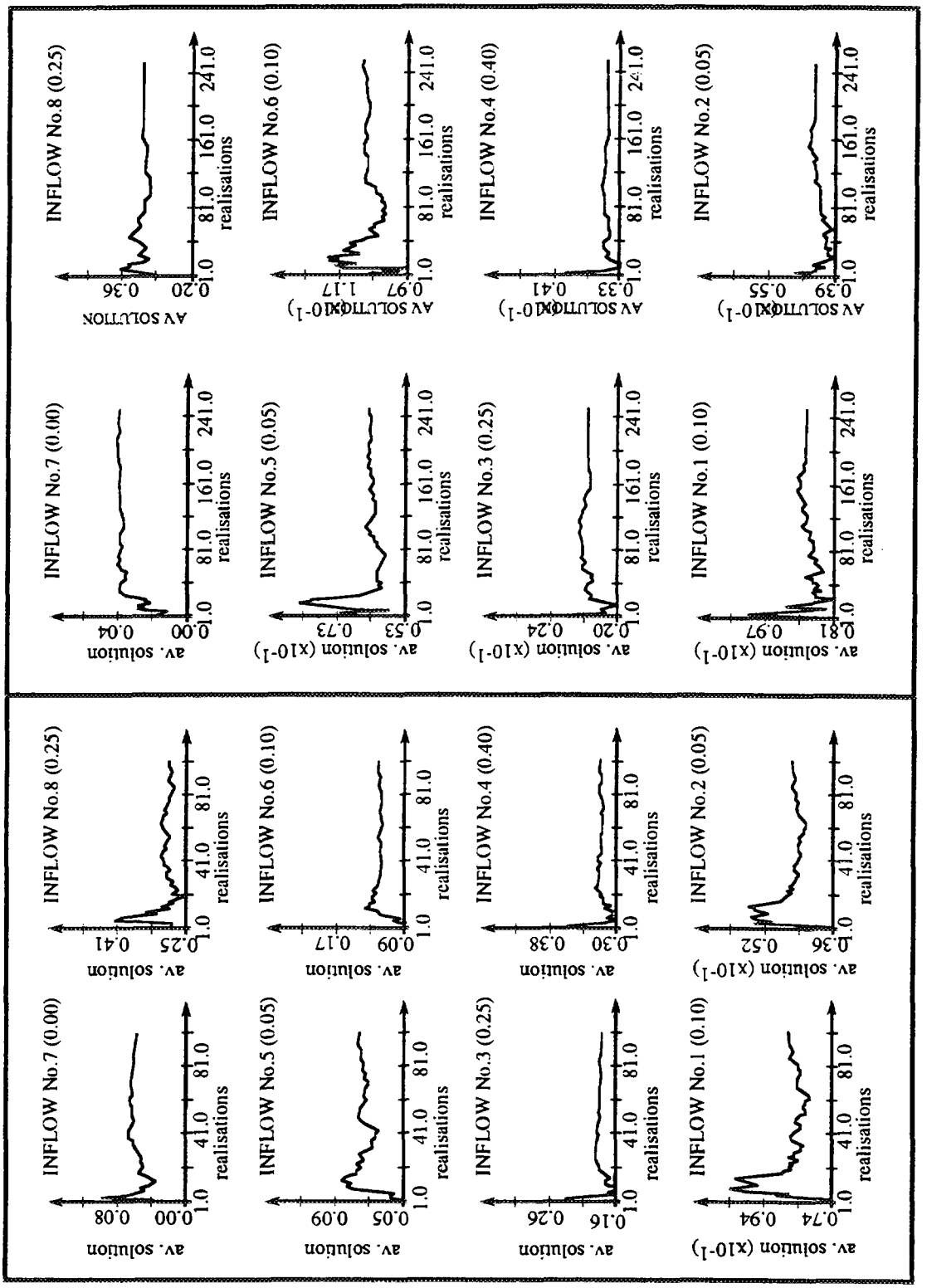

Figure 13: Results of Monte Carlo simulations with β_k values equal to 0.05 (A) and to the coefficient of variation determined from laboratory standards (B).

In a comparison between an analytical solution of the flow equation in one dimension and a solution provided by the mixing cell approach, Van Ommen (1985) deduced that the mixing cell model properly describes the spatial distribution of conservative and reactive tracers.

This model can also assess the spatial distribution of transmissivities providing that piezometric heads can be assigned to every cell and across the flowing boundaries. The results from the southern Arava basin are in a fairly good agreement with transmissivity values obtained by various types of pumping tests. The calculated transmissivities obtained from the aforementioned model are a sort of spatial average values span over the region across every flowing boundary between adjacent cells. This eliminates the vast variability caused by local (usually unknown) non homogeneous geological structures that heavily affects the results obtained by pumping tests.

The fact that the model yields good results when noisy data satisfy constraints similar to those that real data usually satisfy, suggests that the model should be able to deal with real hydrologic conditions. While errors in measured concentrations affect the estimation of fluxes, inaccurate information on the configuration and dimensions of cells, and on the hydraulic head temporal and spatial distribution has extreme influence on the evaluated transmissivities. With the above-mentioned limitations, the model seems to be very sensitive to the quality of the collected data. Deviations from the chemical and isotopic constraints yield an unbounded solution indicating either errors in input data or misunderstandings of the groundwater flow pattern, sources, and processes of aquifer recharge (Adar, 1984).

REFERENCES

Adar, E., 1984. Quantification of aquifer recharge distribution using environmental isotopes and regional hydrochemistry. Dissertation, University of Arizona, Tucson, Arizona, 251 pp.

Adar, E.M. and S.P. Neuman (1986). "The use of environmental tracers (isotopes and hydrochemistry) for quantification of natural recharge and flow components in arid basins". The 5th International Symposium on Underground Tracing, Athens, Greece, pp. 235-253.

Adar, E.M., Neuman, S.P. and Woolhiser, D.A., 1988. Estimation of spatial recharge distribution using environmental isotopes and hydrochemical data. I. Mathematical model and application to synthetic data. Journal of Hydrology, 97, pp. 251-277.

Adar, E.M. and Neuman, S.P., 1988. Estimation of spatial recharge distribution isotopes and hydrochemical data. II. Application to Aravaipa Valley in Southern Arizona, USA. Journal of Hydrology, 97, pp. 297-302.

Adar, E. and S. Sorek (1989). "Multi-compartmental modelling for aquifer parameter estimation using natural tracers in non-steady flow." Advances in Water Resources, Vol. 12, pp 84-89.

Adar, E.M., and S. Sorek (1990). " Numerical method for aquifer parameter estimation utilizing environmental tracers in a transient flow system". MODELCARE 90, International Conference on Calibration and Reliability in Groundwater Modelling, The Hague, Holland, K. Kovar, Ed. IAHS Pub. No. 195, pp 135-148.

Adar, E., E. Rosenthal, A.S. Issar and O. Batelaan. (1992) "Quantitative assessment of flow pattern in the southern Arava Valley (Israel) by environmental tracers in a mixing cell model." Journal of Hydrology Vol. 136, PP 333-354.

Bard, Y., 1974. Nonlinear Parameter Estimation (Appendix D). Academic Press, 332 pp.

Belan, R.A., 1972. Hydrogeology of a portion of the Santa Catalina mountains. M.S. Thesis, University of Arizona, 68 pp.

Besbes, M., Delhomme, J.P. and DeMarsily, G., 1978. Estimating recharge from ephemeral streams in arid regions: A case study at Kariouan, Tunisia. Water Resour. Res., 14(2), pp. 281-290.

Blake, G., Schlichting, E. and Zimmerman, M., 1973. Water recharge in a soil with shrinkage cracks. Soil Science Society of America Proceedings, 37, pp. 669-672.

Bos, M.G. and Nugteren, J., 1974. On irrigation efficiencies. International Institute for Land Reclamation and Improvement, Publication 19. Wageningen, The Netherlands, 89 pp.

Box, G.E.P. and E. Muller, E., 1974. A note on the generation of random normal deviates. Ann. Math. Statist., 29, pp. 610-611.

Bredenkamp, D.B., Schulte, J.M. and Du Toit, G.J., 1974. Recharge of a dolomite aquifer as determined from tritium profiles. Proc., IAEA, Vienna, pp. 73-94.

Briggs, P.C. and Werho, L.L., 1966. Infiltration and recharge from the flow of April 1965 in the Salt river near Phoenix, Arizona. Arizona State Land Department, Water Resources Report No. 29, 12 pp.

Burkham, D.E., 1970. Depletion of stream flow by infiltration in the main channels of the Tucson Basin, Southeastern Arizona. U.S. Geological Survey, Water Supply Paper 1939-B, 36 pp.

Campana, M.F. and Simpson, E.S., 1984. Groundwater residence times and discharge rates using discrete-state compartment model and ^{14}C data. J. Hydrol. 72, pp. 171-185.

Campana, M.F. and Mahin, D.A., 1985. Model - derived estimates of groundwater mean ages, recharge rates, effective porosities and storage in limestone aquifer. Journal of Hydrology, pp. 247-264.

Carrera, J. and Neuman, S.P., 1986a. Estimation of aquifer parameters under transient and steady-state conditions. I. Maximum likelihood method incorporating prior information. Water Resour. Res., 22(2), pp. 201-211.

Carrera, J. and Neuman, S.P., 1986b. Estimation of aquifer parameters under transient and steady-state conditions. II. Uniqueness, stability and solution algorithms. Water Resour. Res., 22(2), pp. 211-227.

Carrera, J. and Neuman, S.P., 1986c. Estimation of aquifer parameters under transient and steady-state conditions. III. Application to synthetic and field data. Water Resour. Res., 22(2), pp. 228-242.

Dincer, T., Al-Mugrin, A. and Zimmerman, M., 1974. Study of the infiltration and recharge through the sand dunes in arid zones with special reference to the stable isotopes and thermonuclear tritium. J. Hydrol., 23, pp. 79-109.

Duffy, C.J., Gelhar, L.W. and Gross, G.W., 1978. Recharge and groundwater conditions in the western region of the Roswell Basin. Partial technical completion report, Proj. No. A-005-NMEX, New Mexico Water Resources Research Institute, Las Cruces, New Mexico.

Eakin, T.E., 1966. A regional interbasin groundwater system in the White River area, Southern Nevada. Water Resour. Res. 2(2), pp. 251-272.

Flug, M., Abi-Ghanem, G.V. and Duckstein, L., 1980. An event-based model of recharge from an ephemeral stream. Water Resour. Res., 16(4), pp. 685-690.

Feth, J.H., Barker, D.A., Morre, L.B. Brown, R.J., and Veirs, C.E., 1966. Lake Bonneville: Geology and hydrology of the Weber Delta District, including Ogden, Utah. U.S. Geological Survey, Professional Paper 518, 76 pp.

Gat, J.R., and Dansgaard, W., 1972. Stable isotope survey of the fresh water occurrence in Israel and the Jordan rift Valley. J. Hydrol., 16, 177-211.

Gelhar, L.W., 1974. Stochastic analysis of phreatic aquifers. Water Resour. Res., 10(3), pp. 539-545.

Gorelick, S.M., Evans, B. and Remson, I., 1983. Identifying sources of groundwater pollution: An optimization approach. Water Resour. Res., 19(3), pp. 779-790.

Heerman, D.F. and Kincaid, D.C., 1974. Scheduling irrigation with a programmable calculator. Agricultural Research Service, ARS-NC-12.

Howard, K.W.F. and Lloyd, J.W., 1979. The sensitivity of parameters in the Penman evaporation equations and direct recharge balance. J. Hydrol., 41, pp. 329-344.

Issar, A., 1983. On the source of water from the thermomineral springs of Lake Kinneret (Israel). J. Hydrol., 60, 175-183.

Issar, A. and Gat, J., 1981. Environmental isotopes as a tool in hydrogeological research in arid basin. Ground Water, 19(5), pp. 490-494.

Issar, A. and Gilad, D., 1982. Groundwater flow systems in the arid crystalline province of southern Sinai. Hydrol. Sci. J., 27, pp. 309-325.

Jacob, C.E., 1943. Correlation of groundwater levels and precipitation on Long Island, New York, I. Trans. Amer. Geophys. Union, 24, pp. 564-573.

Jacob, C.E., 1944. Correlation of groundwater levels and precipitation on Long Island, New York, II. Trans. Amer. Geophys. Union, 25, pp. 928-939.

Kafri, U. and Ben-Asher, J., 1978. Computer estimates of natural recharge through soils in southern Arizona, U.S.A. J. Hydrol., 38, pp. 125-138.

Karmeli, D., Salazar, L.J. and Walker, W., 1978. Assessing the spatial variability of irrigation water applications. U.S. Environmental Protection Agency, EPA-6000/2-78-041, 201 pp.

Keith, S.J., 1981. Stream channel recharge in the Tucson Basin and its implications for ground water management. M.S. Thesis, Tucson, Arizona, University of Arizona.

King, T.G. and Lambert, J.R., 1976. Simulation of deep seepage to a water table. Trans. Amer. Soc. Agr. Eng., 19, pp. 50-54.

Lawrence, F.W. and Upchurch, S.B., 1982. Identification of recharge areas using geochemical factors analysis. Ground Water, 20(6), pp. 260-287.

Levin, M., Gat, J.R. and Issar, A., 1980. Precipitation, flood- and groundwaters of the Negev highlands: An isotopic study of desert hydrology. Proc., IAEA, Vienna, pp. 3-22.

Leggette, R.M., 1936. Note in Trans. Amer. Geophys. Union, 17, pp. 341-344.

Marsh, J.A., 1968. The effect of suspended sediment and discharge on natural infiltration of ephemeral streams. M.S. Thesis, University of Arizona, Tucson, Arizona, 42 pp.

Matlock, W.G., 1965. The effect of silt-laden water on infiltration in alluvial channels. Ph.D. dissertation, University of Arizona, Tucson, Arizona, 102 pp.

Matlock, W.G., 1970. Mathematical analysis of ground water recharge. Trans. Amer. Soc. Civil Eng., 13(6), pp. 785-791.

Matlock, W.G. and Davis, P.R., 1972. Groundwater in the Santa Cruz Valley, Arizona. Technical Bull. 194, University of Arizona, Agricultural Experiment Station, Tucson, Arizona, 37 pp.

Mazor, E., 1982. Rain recharge in the Kalahari - A note on some approaches to the problem. J. Hydrol., 55, pp. 137-144.

Mazor, E., Verhagen, B.T., Senschop, J.P.F., Robins, N.S. and Hutton, L.G., 1974. Kalahari groundwaters: Their hydrogen, carbon and oxygen isotopes. In: Isotope Techniques in Groundwater Hydrology, Proc., IAEA, Vienna, pp. 203-223.

Mero, F., 1963. Application of the groundwater depletion curves in analyzing and forecasting spring discharges influenced by well fields. Intern. Assoc. Sci. Hydrol. Publication No. 63, pp. 107-117.

Moench, A.F. and Kisiel, C.C., 1970. Application of the convolution relation to estimating recharge from an ephemeral stream. Water Resour. Res., 6(4), pp. 1087-1094.

Olmstead, F.H., Loeltz, D.J. and Irelan, B., 1973. Water resources of Lower Colorado River-Salton Sea area. U.S. Geological Survey, Prof. Paper 486-H.

Plummer, L.N., Jones, B.F., and Truesdell, A.H., 1976. WATEQF - A fortran IV version of WATEQ, a program for calculating chemical equilibrium of natural waters. U.S. geological Survey, Nat. Tech. Info. Serv., PB 261027, 61 pp.

Plummer, L.N., Prestemon, E.C., and Parkhurst, D.L., 1991. An interactive code (NETPATH) for modeling net geochemical reactions along a flow path. U.S. Geological Survey, Water Resources Investigations Report 91-4078, Reston, Virginia, 93 pp.

Rasmussen, T.C., 1982. Solute transport in saturated fractured media. M.Sc. Thesis, University of Arizona, Tucson, Arizona.

Rantz, S.E. and Eakin, T.E., 1971. A summary of methods for the collection and analysis of basic hydrologic data for arid regions. Open File Report, U.S. Geological Survey Water Resources Division, Menlo Park, California, 125 pp.

Rosenthal, E., Adar, E. Issar, A.S., and Batelaan, O. 1990. Definition of groundwater flow pattern by environmental tracers in the multiple aquifer system of southern Arava valley, Israel. Journal of Hydrology, Vol. 117, PP 339-368..

Shampine, W.J., Dincer, T. and Noory, M., 1979. An evaluation of isotope concentrations in the groundwater of Saudi Arabia. Proc. Isotope Hydrology, 1978. IAEA, Vienna, 2, pp. 443-463.

Simpson, S.E., 1975. Finite state mixing cell models. Bilateral United States - Yugoslavian Seminar in Karst Hydrology and Water Resources, Dubrovnik, 1975.

Simpson, E.S. and Duckstein, L., 1976. Finite state mixing-cell models. In: Karst Hydrology and Water Resources, V. Yevjevish, (ed.), Ft. Collins, Colorado. Water Resour. Publications, 2, pp. 489-508,

Tanji, K., 1977. A conceptual hydrosalinity model for predicting salt load in irrigation return flows. In: Managing Saline Water for Irrigation, H.E. Dregne (ed.). Proceedings of the International Conference on Managing Saline Water for Irrigation, Planning for the Future, Center for Arid and Semi-Arid Land Studies, Texas Tech. University, pp. 49-72.

Thornwaite, C.W. and Mather, J.R., 1957. Instruction and tables for computing potential evapotranspiration and the water balance. In: Publication in Climatology, 10(3), 311 pp.

Van Ommen, H.C., 1985. The "mixing cell" concept applied to transport of non-reactive and reactive components in soils and groundwater. Journal of Hydrology, 78, pp. 201-213.

Venetis, C., 1971. Estimating infiltration and/or the parameters of unconfined aquifers from ground water level observations. J. Hydrol., 12(2), pp. 161-169.

Verhagen, B.Th., Sellschop, J.P.F. and Jennings, C.M.H., 1970. Contribution of environmental tritium measurements to some geohydrological problems in Southern Africa. Proc., IAEA, Vienna, pp. 289-313.

Verhagen, B.Th., Dziembowski, Z. and Oosthuizen, J.H., 1978. An environmental isotope study of a major dewatering operation at Sishen mine, Northern Cape Province. Proc., IAEA, Vienna, pp. 65-81.

Vogel, J.C., Thilo, L. and Van Dijken, M., 1974. Determination of groundwater recharge with tritium. J. Hydrol., pp. 23: 131-140.

Wagner, B.J. and Gorelick, S.M., 1986. A statistical methodology for estimating transport parameters: Theory and applications to one-dimensional advective dispersive systems. Water Resources Research, 22, pp. 1303-1315.

Wagner, B.J. and Gorelick, S., 1986. Optimal groundwater quality management under parameter uncertainty. Water Resources Research, 23, pp. 1162-1174.

Walker, W.R., 1970. Hydrosalinity model of the Grand Valley. M.S. Thesis, Colorado State University, Ft. Collins, Colorado, 75 pp.

Wilmot, C.J., 1977. WATBUG: A FORTRAN IV algorithm for calculating the climatic water budget. Water Resour. Center, University of Delaware, Newark, Delaware, 55 pp.

Wilson, L.G. and DeCook, K.J., 1968. Field observations on changes in the subsurface water regime during influent seepage in the Santa Cruz River. Water Resour. Res., 4(6), pp. 1219-1234.

Wind, G.P. and Van Doorne, W., 1975. A numerical model for the simulation of unsaturated vertical flow of moisture in soil. J. Hydrol., 24, pp. 1-20.

Wolf, P., 1967. Methods of non-linear programming. Chap. 6. In: Interscience, J. Wiley, New York,pp. pp. 97-131.

Woolhiser, D.A., Emmerich, W.E. and Shirley, E.D., 1985. Identification of water sources using normalized chemical ion balances: A laboratory test. J. Hydrol., 76, pp. 205-231.

Woolhiser, D.A., Gardner, H.R. and Olsen, S.R., 1982. Estimation of multiple inflows to a stream reach using water chemistry data. Trans., ASAE, 25(3), pp. 616-622.

Yurtsever, Y. and Payne, B.R., 1978 a. Application of environmental isotopes to groundwater investigation in Qatar. Proc., IAEA, Vienna, pp. 465-490.

Yurtsever, Y. and Payne, B.R., 1978 b. A digital simulation approach for a tracer case in hydrological system (multi-compartmental mathematical model). Int. Conference on Finite Elements in Water Resources, London, 1978.

Yurtsever, Y. and Payne, B.R., 1985., Time-variant linear compartmental model approach to study flow dynamics of a karstic groundwater system by the aid of environmental tritium (a case study of south-eastern karst area in Turkey). Symposium of Karst Water Resources, Ankara-Antalya, July 1985, IAHS Publ. no. 161, pp. 545-561.

Zimmerman, U., Ehhalt, D., and Munnich, K.O., 1967. Soil water movement and evapotranspiration: Changes in the isotopic composition of the water. Isotope in Hydrology, IAEA, Vienna, pp. 567-585.

Zimmerman, U. Munnich, K.O., and Roether, W., 1966. Tracers determine movement of soil moisture and evapotranspiration, Science, 152 (3720), pp. 346-347.